Kirill L. Levine
Telecommunication academy named after S.M. Budienny
Andrey G. Syrkov
St. Petersburg Mining University

BRIEF VIEW TO NEW MATERIALS: PREPARATION AND PROPERTIES IN THE ASPECT OF NANOTECHNOLOGY

Periodic edition Smart Nanocomposite's letters presents new studies in the fast growing area of smart materials, in particular, composite nanostructured materials. It focuses on the physics and physical chemistry of surfaces, interfaces, thin films and coatings, nanoparticles and nanostructures, and their applications. Nanostructured ceramics, alloys, various nanocarbon forms (nanotubes, fullerene, graphene) and their composites used in sensors (including single molecule sensing) and actuators, artificial metabolism, drug delivery, selective membranes, fuel cells, energy storage, and photovoltaics are just a few examples of new classes of materials and applications that are within the scope of this series. It features the results of interdisciplinary research from universities, national labs, and privately owned companies.

Smart Nanocomposite's letters focuses mostly on practical applications of nanodevices, and on proof of the concept publications. Smart Nanocomposite's letters also deals with safety issues: safety of nanotechnology to the environment, controlling the nanodevices, and other aspects.

Smart Nanocomposite's letters is peer reviewed, providing high standards of publication. It is composed on chapters of the highest academic level in their field.

Smart Nanocomposite's letters
published by

Science Impact
SC, U.S.A.

E-mail: science_impact@hotmail.com

ISBN: 9781079785517

Technical director
Rajan Singh
Technical editor
Mikhail Silivanov

Table of contents

SECTION 2 : PREPARATION METHODS AND PROPERTIES MODIFICATION

SECTION 3 : FUNCTIONAL PROPERTIES AND PRACTICAL APPLICATIONS

SHORT COMMUNICATIONS TO EDITOR

MODERN ASPECTS OF NANOPHYSICS AND NANO-ENGINEERING. INTRODUCTORY WORD

Galina K. Elyashevich and Kirill L. Levine

This volume of a series "Nanotechnology science and technology" entitled "Brief view to new materials: preparation, properties and applications in the aspect of nanotechnology" covers a wide field of Material Science including the theoretical and experimental investigations of organic and inorganic systems, methods of preparation, characterization and modification of functional properties and practical applications. It is partially based on materials of a seminar-symposium "Nanophysics and nanomaterials", venue: St. Petersburg Mining University, Nov. 28-29, 2018, St. Petersburg, Russian Federation.

Section 1 ("Theoretical and experimental investigations") included thermodynamic modeling of the behavior of fullerenes at heating in Argon (Barbin) and also a broad analysis of this method as the most effective and rigorous approach to the investigations of complicated chemical and phase transformations occurring in chemical process (Slobodov).

The number of communications describes the structural investigations of a wide variety of materials such as different sorts of steel in grained modification for mining equipment, elements of rock-breaking, crushing and grinding equipment (Bolobov); ceramic materials for treatment in milling (Khalimonenko), investigations of acid-base surface centers of adsorbents based on oil shale (Nazarenko) and polycrystalline phosphor films on nano-SiC (Sergeeva). Surface structural investigations of variety of materials by ellipsometry are also described (Skaletskaya).

In one communication (Nosov) the idea to make the forecasting of the Resource of Structural Materials using their Strength Nano-Characteristics is presented.

The communication of special interest is the study of interaction of Sulfur-Containing Platinum Compound with DNA as a system combining inorganic and biologically active components (Kasyanenko).

Section 2 ("Methods of preparation and properties modification") includes the communications related to preparation methods for the materials containing various components – metals (Drozdov, Khristyuk), metal alloys (Ibragimov) as powders (Kulinich), films (Lushpa) and solid solutions (Nemov), and also polymers and fullerenes (Krasnyy) using a wide set of experimental methods, such as synthesis, casting, electrocrystallization, magneto-abrasive machining (Zlotnikov).

Communications in Section 3 ("Functional properties and practical applications") are focused on the possibility of using new nanomaterials of different composition and design as powders for corundum ceramics (Bogdanov), mechanically strengthened nanomaterials and nanocoatings (Gogolinskii), aluminum boards in LED technology (Muratova) and polymer membranes (Lopatin).

Mentoring aspect - education of the young researchers involved in nanoscience and technology – is covered in communication "Students Training on "Nanoengineering" (Panfilov), which is also a very important and promising scientific field.

SECTION 1 :

THEORETICAL AND EXPERIMENTAL INVESTIGATIONS

THERMODYNAMIC MODELING OF THE HEATING OF C_{32} FULLERENES IN THE ENVIRONMENT OF ARGON

Nick M. Barbin,[1,2,3] Vasiliy P. Dan,[1] Dmitriy I. Terentiev,[1] Sergey G. Alekseev[1,4]

E-mail: NMBarbin@mail.ru

[1]Ural Institute of State Fire Service of Emercom of Russia, Ekaterinburg, Russia
[2]Ural Agrarian State University, Ekaterinburg, Russia
[3]Ural Federal University, Ekaterinburg, Russia
[4]SIC "Reliability and resource of large systems and machines" of the Ural branch of the Russian Academy of Sciences, Ekaterinburg, Russia

ABSTRACT

The behavior of C_{32} fullerene under heating in argon under atmospheric pressure in the temperature range 473...4273 K by the method of thermodynamic modeling using TERRA software was studied.

Keywords: heating, fullerene C_{32}, carbon nanomaterials, thermodynamic modeling, TERRA.

INTRODUCTION

Fullerenes have a number of unique properties, largely depending on their quality, such as: diamagnetic properties, electrical conductivity, high strength in combination with high values of elastic deformation [1]. Their presence is determined by high strength of carbon-carbon bonds, colossal strength of atomic packing, and slightly low density of structure defects [2]. In this paper, the behavior of C_{32} fullerenes under heating in argon is studied by thermodynamic modeling. The calculation used thermodynamic parameters of condensed carbon fullerene C_{32} [3] and gaseous C, C_2, C_3, C_4, C_5, C_{28}, C_{32}, C_{44}, C_{50}, C_{56}, C_{60}, C_{70}, C_{76}, C_{84}, C_{90} and C_{94} [4]. Temperature range-from 473 K to 4273 K; pressure 0.1 MPa. The ratio of argon to carbon is 1:4.

METHOD

Thermodynamic modeling includes thermodynamic analysis of the equilibrium state of the system as a whole [5]. The calculations were made by the TERRA software package, which is a stage of further development of the ASTRA software package.

Calculations of the composition of the phases and characteristics of the equilibrium using reference databases are performed in [6, 7].

Thermodynamic modeling has been successfully applied in [8, 9].

EXPERIMENTAL SECTION

The content of condensed fullerene C_{32} in the C_{32}-Ar system is unchanged in the temperature range of 473…2673 K and is 0,520 mol/kg. In the temperature range of 2673...3873 K the content of C_{32} decreases to almost 0. The decrease in the content of condensed fullerene by the beginning of the process of sublimation of the condensed fullerene of the system and the appearance of gaseous C, C_2, C_3, C_4, C_5 in the system is accompanied.

The content of gaseous C and C_2 increases to a temperature of 4273 K; reaches 2,178 mol/kg and 1,391 mol/kg.

The content of gaseous C_3 is increased to a temperature 3873 K; reaches 4,253 mol/kg at a temperature 3873 K the observed inflection point. In the temperature interval 3873…4273 K water vapor content is reduced to 3,650 mg/kg.

The vapor content of C_4 and C_5 increases to a temperature of 3873 K and reaches 0,075 mol/kg and 0,332 mol/kg. In the temperature range 3873...4273 K, the gaseous content of C_4 and C_5 decreases linearly to 0,054 mol/kg and 0,105 mol/kg, respectively.

CONCLUSION

The bending points on the curves of the degree of transformation of reactions of the C_{32}-Ar system, which correspond to the phase transition of carbon, as well as changes in the phase compositions, are determined.

References

[1] Ballade.R. F. A. Lewis, Graphite and its crystal compounds / Translation from English. E. S. Golovina, O. A. Tsukanova. - M.: Mir, 1965.- 257 p.

[2] Bells S. N. Carbon-based materials. Properties, technologies, applications: educational. village-Dolgoprudny: publishing House "Intellect", 2012. - 296 p.

[3] Moiseev G. K., Vatolin N. Ah. Evaluation of thermodynamic properties of a number of condensed carbon compounds / / Journal of physical chemistry. - 2002. - Vol. 76. - №3. – P. 424-428.

[4] Moiseev G. K., Vatolin N. Ah. Thermodynamic properties of some gaseous fullerenes / / Journal of physical chemistry. - 2002. - Vol. 76. - №2. - P. 217-220.

[5] Vatolin N. A. Moiseev G. K., Trusov B. G. Thermodynamic modeling in high temperature systems. M.: Metallurgy, 1994. 352 p.

[6] Moiseev G. K., Vatolin N. Ah. Computer modeling of formation of various condensed forms of carbon / / Journal of physical chemistry. - 2002. - Vol. 76. - №8. – Pp. 1366-1370.

[7] Moiseev G. K., Vatolin N. Ah. Assessment of the standard enthalpy of formation (sea) of condensed metastable "small" carbon self-associates and some metals // Reports of the Academy of Sciences. - 2003. - Vol. 392. - №5. - P. 653-656.

[8] Barbin Nick M., Dan Vasily P., Terentyev Dmitry I., Alekseev Sergey Grigoryevich modeling of behavior of carbon nanoparticles of C44 at heating in the atmosphere of argon. computer experiment. - Smart Nanocomposites 2016. Volume 7 Issue 1. P. 1-7.

[9] Barbin Nick M., Dan Vasily P., Terentyev Dmitry I., Alekseev Sergey G. thermodynamic modeling of higher fullerenes C84 under heating in an inert atmosphere. - Smart Nanocomposites 2016. Volume 7 Issue 2. P. 251-257.

INFLUENCE OF THE STRUCTURE OF CERAMIC MATERIAL OF A TOOL ON THE QUALITY OF TREATMENT IN MILLING

Khalimonenko A.D., Gorshkov I.V.

Khalim76@rambler.ru
Saint Petersburg Mining University

ABSTRACT

The paper discusses the problems that arise when milling high-precision flat surfaces with a tool equipped with ceramic cutting plates. The research results showed that the quality of processing and tool life during finishing milling depends on the parameters of the structure of the ceramic tool. According to the research results, a method for determining the parameters of the structure of a ceramic tool is proposed.

Keywords: cutting ceramics; tool life; milling; processing quality; mounting face.

GOALS

The purpose of this work is to determine the durability of ceramic tools, affecting the quality of processing when milling the exact elements of machine parts, based on the structural parameters of the tool material.

INTRODUCTION

Modern production seeks to apply new technologies and tool materials that have the best cutting properties and provide the specified quality requirements for processing the precise surfaces of machine parts, being highly resistant to wear. Such precise surfaces are, for example, machine bed shears, made of high-strength gray graphite iron, to which rather high requirements are made to ensure the required dimensional accuracy, roughness, geometric accuracy requirements of the elements and their mutual arrangement [1].

Modern technology for processing such surfaces is consistent rough, semi-finishing and finishing milling. Finishing milling is recommended to be carried out with mills equipped with interchangeable ceramic cutting plates. This technology allows you to

achieve the highest quality surface treatment with maximum performance, but it is not without drawbacks, since the low stability of cutting ceramics with intermittent cutting leads to an early failure of the tool [1].

When one of the ceramic plates fails to work, the load on the other plates increases, the tool quickly fails, which immediately leads to a loss in quality of processing. It follows that the task of this study is to determine the performance of all ceramic plates in order to equip the cutters with such ceramic plates, the resistance of which is at the same level [1, 2].

MATERIALS AND METHODS

The oxide-carbide type ceramics is manufactured on the basis of aluminum oxide and titanium, tungsten and molybdenum carbides by hot pressing. The performance of cutting ceramics, especially the durability of the tool, is influenced by the parameters of the material structure, of which the most important are the number of carbide grains and their average diameter. Ceramic plates with a finer-grained structure (average grain size of $1.2...1.5 \cdot 10^3$ nm) and a smaller percentage of porosity (about 8%) have a greater performance as compared to ceramic plates, in which the structure consists of grains of large diameter (average grain size $1.9...2.5 \cdot 10^3$ nm) and there is a relatively large percentage of porosity (about 12%) [2, 3].

The selection of ceramic plates for milling according to their performance was made by the correlation dependence of the structural parameters and the electrical resistivity of the material. Ceramic plates with a larger structure have specific electrical resistivity values close to R = 10 Ω, and ceramic plates with a smaller microstructure have electrical resistivity parameters close to R = 100 Ω [4]. A similar range of parameters of the electrical resistivity of ceramic plates allows them to be in the same group in terms of their microstructural parameters and performance parameters [4].

For the experiments, an end mill was used and the recommended finishing modes adopted for the standard technology of the mounting faces were selected.

RESULTS AND DISCUSSION

As part of this research, a series of experiments was carried out in which a mill equipped with ceramic plates with similar electrical resistivity parameters (plate group with R = 75...100 Ω) showed the following results of the stability of the machining process using the milling method: the actual tool path without loss of machining quality amounted to l =

32 m, after which there was a sharp deterioration in the roughness of the treated surface and going beyond the tolerance of the processed element, the actual period of durability of the tool when it could work without loss of quality was T = 35.6 min [5].

The research of the processed surface showed that until the instrument reached the limit of working capacity, the quality of the machining was within the limits sufficient for parts of this type - the surface roughness was not lower than Ra = 1.6 μm, flatness deviations did not exceed 0.03 mm over a length of 100 mm.

In the second series of experiments, one of the cutter plates was chosen in such a way that its working capacity and electrical resistivity would sharply differ among the representatives of the group (R = 10 Ω). The tests have shown that the path traveled by the tool without loss of quality of processing and the actual period of resistance was reduced by 1.5 times.

CONCLUSION

Thus, we can conclude that the structure of the cutting ceramic material of the same brand is not the same, and this has a decisive influence on the durability and performance of the ceramic cutting tool.

That is why the determination of the structure of the ceramic tool at the preproduction stage can significantly improve the processing stability and increase the tool's working efficiency, while ensuring the required quality of machining the exact surfaces of the machine parts. The parameters of the structure of ceramic plates with high accuracy allows you to determine the method of measuring the electrical resistivity.

Based on this, it is recommended to equip a multi-blade cutting tool with such ceramic plates, the performance criteria of which are in the same group. To increase the service life of a tool equipped with cutting ceramics, to increase processing performance and to ensure the required quality indicators, it is desirable to install such ceramic plates into the tool, whose electrical resistivity values approach R = 100 Ω.

Testing of new methods for determining the performance of ceramic plates is currently underway, in particular by the eddy current method and based on the Hall effect.

REFERENCES

[1] Maksarov V., Khalimonenko A. Quality assurance during milling of precision elements of machines components with ceramic cutting tools. International Review of Mechanical Engineering, Praise Worthy Prize, 2018, Vol. 12(5), P. 437-441.

[2] Maksarov V., Khalimonenko A., Olt J. Managing the process of machining on

machines on the basis of dynamic modelling for a technological system. Építőanyag – Journal of Silicate Based and Composite Materials, Scientific Soc Silicate Industry - SZTE, 2017, Vol. 69(2), P. 66-71.

[3] Maksarov V., Khalimonenko A., Olt J. Effect of porosity on the performance of cutting ceramics / Agronomy Research, Tartu: Estonian University of Life Sciences, 2016, Vol. 14, SI 1, P. 1043-1052.

[4] Maksarov V., Khalimonenko A. Forecasting performance of ceramic cutting tool. Key Engineering Materials, Trans Tech Publications, 2017, Vol. 736, P. 86-90.

[5] Maksarov V., Khalimonenko A., Timofeev D. Machining quality when lathing blanks with ceramic cutting tools. Agronomy Research, Tartu: Estonian University of Life Sciences, 2014, Vol. 12, P. 269-278.

STUDY OF ACID-BASE SURFACE CENTERS OF ADSORBENTS BASED ON OIL SHALE OF LENINGRAD DEPOSIT

M.Yu. Nazarenko, S.N. Saltykova*

E-mail: max.nazarenko@mail.ru
Department of Processing mineral raw materials, St. Petersburg Mining university, Russia

ABSTRACT

In this paper, the study of the distribution of acid-base centers on the surface of adsorbents made from oil shale of the Leningrad field. The results of studying the micro - and nanopores properties of these adsorbents are presented. The results indicate that they may be used as fillers in polymer composites, filter materials, and sorbents. The surface of oil shales is characterized by the presence of centers with p*K*a = +1.5, p*K*a = +3.5, p*K*a = +6.4, p*K*a = +9.5, and p*K*a = +14.2. At the surface of shale ash, we find centers with p*K*a = +1.5, p*K*a = +4.1, p*K*a = +6.4, p*K*a = +9.5, and p*K*a = +14.2. The presence of acidic and basic Bronsted centers indicates sorptional activity with respect to organic pollutants (petroleum and its products, for example) and ionic heavy metals.

Keywords: oil shale, adsorbent, pores, surface area, micropore

INTRODUCTION

Oil shales are promising for use in the power, chemical, and coke industries. In contrast to other solid fossil fuels, oil shales contain considerable quantities of hydrogen in their organic matter and a large proportion of mineral components [1]. To determine suitable applications for oil shales, we need information regarding their chemical and mineralogical composition, the structure of the organic matter, and the changes at different stages of thermal and chemical treatment. Oil shales from the Baltic Basin contain up to 50% mineral impurities (including SiO_2, Al_2O_3, CaO, and Fe_2O_3), as established in [2-3]. In mineral composition, oil sales are similar to natural minerals such as quartz sand, zeolite, or shungite, which are used for filtration or sorption. In the present work, we determine the surface reactivity of oil shales and shale ash.

The donor–acceptor reactivity of the surface may be characterized by the acid–base properties, which are related to practically all the fundamental parameters of a solid. Therefore, if we determine the composition and content of the active centers, we may predict the reactive and sorption properties of solids used as catalysts and as fillers in polymer composites, filter materials, and sorbents [4-5]. To this end, we determine the distribution and content of acid–base centers at the surface of oil shales and shale ash; and we study the surface area of the material and the distribution of micro- and macropores.

EXPERIMENTAL

We study oil shale of Leningrad deposit (< 0,125 mm fraction) and also oil shale ash (<0,125 mm fraction).

To determine the distribution and concentration of acid–base centers at the surface of oil shales and shale ash, we use the indicator method. By that means, we may investigate the distribution of surface centers and the correlation between the adsorption by specific surface centers and the activity of the surface as a whole. The indicator method is based on the adsorption of monobasic indicators from an aqueous medium by a solid surface. In analytical conditions, the indicator is adsorbed both at Bronsted centers and at Lewis centers, where water molecules are adsorbed by a coordination mechanism in accordance with the corresponding p*K*a value. As a result, quantitative determination gives the total content of Lewis and Bronsted centers of the corresponding strength at the surface of the oil shales and shale ash.

The specific surface area and micro- and nano- pores of oil shale and oil shale ash were conducted on the analyzer, specific surface NOVA3200e.

RESULTS AND CONCLUSIONS

The following conclusions follow from the distribution of acid–base centers at the surface oil shales and shale ash.

1. The surface of oil shales is characterized by the presence of centers with p*K*a = +1.5, p*K*a = +3.5, p*K*a = +6.4, p*K*a = +9.5, and p*K*a = +14.2.

2. At the surface of shale ash, we find centers with p*K*a = +1.5, p*K*a = +4.1, p*K*a = +6.4, p*K*a = +9.5, and p*K*a = +14.2.

3. The presence of acidic and basic Bronsted centers (p*K*a = +1.5, p*K*a = +3.5, p*K*a = +6.4) and the shale ash (p*K*a = +1.5, p*K*a = +4.1, p*K*a = +6.4) indicates sorptional activity of the oil shales and shale ash with respect to organic pollutants (petroleum and its products, for example).

4. The peaks with p*K*a = +9.5 and p*K*a = +14.2 (in the region of basic Bronsted centers) indicate sorptional activity of the oil shales and shale ash with respect to ionic heavy metals.

It is established that oil shale ash (51,796 sm^2/g) has a specific surface area higher than that of oil shale (9,427 sm^2/g), which is mainly due to the fact that during heat processing, a large amount of volatile components thereby increasing the porosity.

The average diameter of the pores of oil shale is in the limit of 8,962 nm - 21,244 nm.

REFERENCES

[1] Leimbi Merike R., Tiina H., Eneli L., Rein K. Composition and properties of oil shale ash concrete / Oil Shale. 2014. Vol. 31, №. 2. 147–160.

[2] Bityukova L., Motler R. Composition of oil shale ashes from pulverized firing and circulating fluidized-bed boiler in Narva thermal power plants / Oil shale. 2010. vol. 27. № 4. 339–353.

[3] Swift T., Mayer S. Study of thermal conversion of oil shale under N_2 and CO_2 atmospheres / Oil shale. 2010. vol. 27. № 4. 309–320.

[4] Nazarenko M.Yu., Bazhin V.Yu., Saltykova S.N., Konovalov G.V. Physicochemical properties of fuel shale / *Coke and Chemistry.* 2014. №3. 44-49;

[5] Nazarenko M.Yu., Kondrasheva N.K., Saltykova S.N. Surface reactivity of fuel shales from the Baltic basin/ *Coke and Chemistry*. 2016. №5. 33-37.

FEATURES OF THE STRUCTURE POLYCRYSTALLINE PHOSPHOR FILMS ON SI (NANO-SIC)

Nina M. Sergeeva, *Sergei P. Bogdanov

*E-mail:Alnserg41@mail.ru
Department of Theoretical Foundations of Materials Science, Saint- Petersburg State Institute of Technology (Technical University), Russian Federation

ABSTRACT

Polycrystalline $Cd_{(1-x-y-z)}(Cu_yAg_z)Zn_xS$ phosphor films were grown in an aqueous colloidal solution of zinc acetate compounds, cadmium nitrate and sodium sulfide on a monocrystalline silicon substrate with a buffer layer of nanocrystalline silicon carbide under normal conditions. The method of scanning electron microscopy (SEM) in the modes of secondary and reflected electrons with different magnifications studied the morphology of the surface of the film, detected particles of different shapes: needle, oval, filamentous and their distribution on it.

Keywords: polycrystalline film, phosphor, particle shape: needle, oval, filamentous.

INTRODUCTION

The combination of good optical properties of phosphors based on solid solutions of cadmium sulfide and zinc [1] and a silicon substrate (Si) with a buffer layer of silicon nanocarbide (SiC) grown on the principle of chemoepitaxial self-assembly of substituting atoms [2, 3] can open new prospects for the synthesis of light-emitting crystals.

METHOD

The finished substrates Si/(nano - SiC) [2,3] were placed in a Petri dish, poured with a certain amount of an aqueous colloidal phosphor solution synthesized according to the procedure [1], and kept in it. Then, after drying, the morphology, peculiarities (features) of the surface structure, and the dispersion composition of the particles of polycrystalline films were studied.

EXPERIMENTAL SECTION

Figure 1 a-h shows micrographs of SEM images of the surface of a polycrystalline phosphor film with magnification from $x10^2$ to $x10^4$ with characteristic morphological formations. These are particles of different shapes: needle, oval, filamentous.

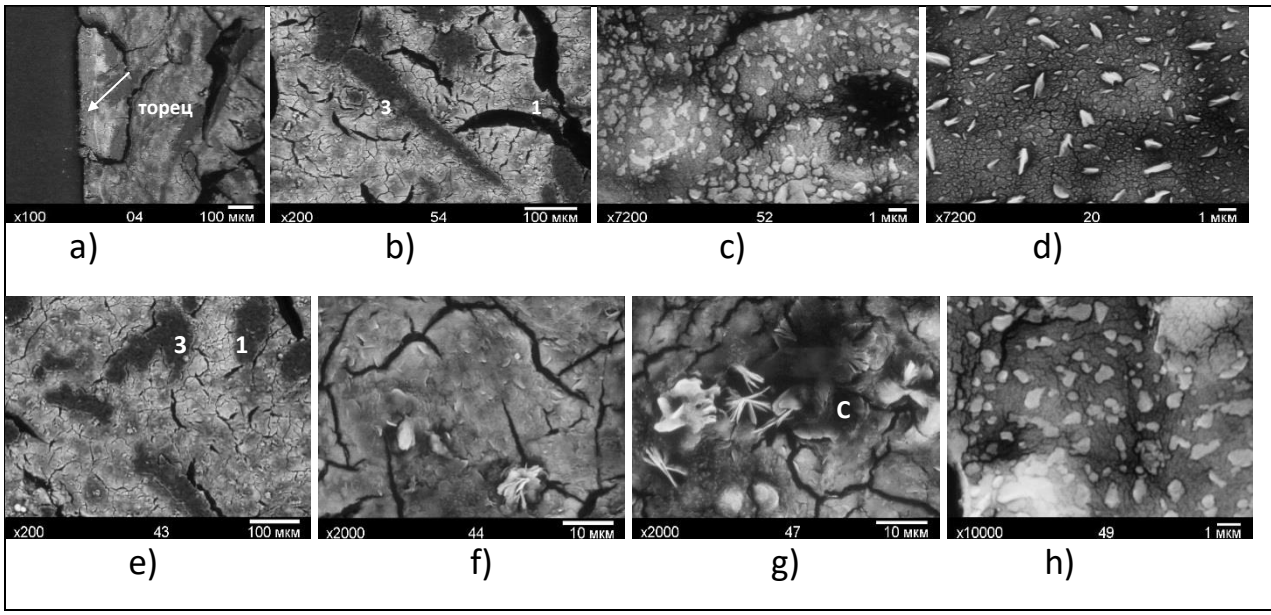

Figure 1. Images –SEM sections of the surface of the phosphor film.

CONCLUSION

Using the SEM method, it is shown that the particles of the film are deposited on the substrate not randomly, but they self-organize in a certain way, adapting to the local rates of heat and mass transfer.

REFERENCES

[1]Sergeeva N.M., Bogdanov S.P. Optical properties control of

Cd1-xZnxS phosphor containing copper, silver, manganese-based alloying metal pairs // Optical J (2017) 84: P. 70 – 79.

[2]Kukushkin S.A., Osipov A.V. New method of solid-phase epitaxy of siliconcarbide on silicon: model and experiment // FTT (2008) 50: P.1188-1195.

[3] Kukushkin S.A., Osipov A.V. Topical Review. Theory and practice of SiC growth on Si and its applications to wide-gap semiconductor films // J Phys. D : Appl. Phys. (2014) 47: P. 313 001.

INTERACTION OF SULFUR-CONTAINING PLATINUM COMPOUND WITH DNA MOLECULE IN SOLUTION.

Sharikhina Yu. V. [1, a)] ***and Kasyanenko N. A.*** [2, b)]

[1]Sharikhina_YuV@pers.spmi.ru
[2] nkasyanenko@mail.ru
[a)]General and Technical Physics Department, Saint-Petersburg Mining University, Russia
[b)] Department of Molecular Biophysics and Polymer Physics, Saint-Petersburg State University, Russia

ABSTRACT

It was demonstrated that DMSO molecule blocks one of the active centers of the platinum compound participating in the formation of coordination bonds with macromolecule. DNA nitrogen groups cannot substitute DMSO molecule in the first coordination sphere of platinum.

Keywords: Calf thymus DNA, Platinum Compounds, Dimethyl Sulfoxide, Circular Dichroism, Fluorescent Microscopy, Hydrodynamic Properties.

INTRODUCTION

Cis-DDP is anticancer drug successfully used in clinical practice [1]. However its disadvantages call for a search of its effective substitutes [2]. While transported to nuclear DNA cis-DDP may interact with sulfur-containing amino acids in the structure of proteins [3]. Such complexes can block cis-DDP active centers and improves the transport ability of the drug [4]. We have evaluated DNA interaction with platinum compound [Pten Cl $SO(CH_3)_2$] NO_3 (Pten (DMSO)) compared with PtenCl_2 (Pten). Pten is a cis-DDP analog that contains ethylenediamine as bidentate ligand in the first coordination sphere of platinum instead of two ammonia molecules. DMSO is characterized by its high ability to penetrate biological membranes. It is used as a solvent for many platinum-based drugs.

METHOD

Flow birefringence, viscometry, fluorescent microscopy (FM), atomic force microscopy (AFM), circular dichroism (CD).

EXPERIMENTAL SECTION

Platinum compounds have been synthesized at the St. Petersburg Technological Institute with the help of Dr. Spevak V. N. The calf thymus DNA (Sigma) and T4 phage

DNA (Sigma) was used. Our experiments have shown that injection of DMSO to the first coordination sphere of Pten instead one atom of chlorine significantly changes the complexation of this compound with a DNA molecule. CD spectra were recorded using a Jobin-Yvon Mark-IV dichrograph. The study of DNA hydrodynamic properties after complexation with Pten and Pten (DMSO) has shown that platinum compounds form a coordination bond with DNA. The difference in binding of Pten (DMSO) and Pten does not show in the degree of binding, but in the final structure of the formed DNA-Pt complex. The volume of DNA molecule varies practically equally after DNA interaction with Pten, Pten (DMSO) and cis-DDP. Viscometry data demonstrate that DNA complexation with cis-DDP, Pten, Pten (DMSO), and trans-DDP is not accompanied by a change of the DNA persistent length. Pten (DMSO) forms one coordination bond with N7 guanine, whereas Pten forms two bonds. Fluorescence images of T4 phage DNA bound with dye (Yo-Yo1) molecules in a solution were observed using Karl Zeiss Axiolab microscope. Experiment was conducted in Moscow State University with the help of Dr. Abramchuk S. S. FM data are compatible with the viscometry data (at the increase of the C_{Pt}/C_{DNA} value the DNA linear dimensions are reduced). The AFM images were taken with a Nanoscope IV MultiMode System (Veeco, USA) operating in contact mode. Silicon tips were used for imaging in air. Before DNA fixation on mica surface initial solution were mixed with $MgCl_2$. FemtoScan Online 1.6 (Advanced Technologies Center, 103009, Russia, Moscow, Bolshaya Nikitskaya Street, 24-7) software was used for analysis of the AFM data [5]. DNA complexation with Pten show tendency for appearance of DNA bending as cisDDP. DNA-PtenDMSO complexes AFM images indicate an existence of intra- or interstrand cross-links as trans-DDP.

CONCLUSION

The injection of DMSO molecules in the first coordination sphere of platinum changes the nature of compound interaction with DNA. DMSO blocks one of the active centers of the platinum complex participating in the formation of a coordination bond. N7 guanine cannot substitute DMSO molecule in the first coordination sphere of platinum.

REFERENCES

[1] B. Rosenberg, L. Van Camp, J. E. Trosko, V. N. Mansour, Platinum compounds: a new class of potent antitumour agents // Nature. 222 (1969) 385-386.

[2] Z. H. Siddik, Cisplatin: mode of cytotoxic action and molecular basis of resistance // Oncogene. 22 (2003) 7265-7279.

[3] J. Reedijk, Why does cisplatin reach guanine-N7 with competing S-donor ligands available in the cell? // Chem. Rev. 99 (1999) 2499-2510.

[4] K. J. Barnham, M. I. Djuran, P. S. Murdoch, J. D. Ranford, P. J. Sadler, l-Methionine increases the rate of reaction of 5-guanosine monophosphate with anticancer drug cisplatin: mixed-ligand adducts and reversible methionine binding // J. Chem. Soc., Dalton Trans. (1995) 3721-3726.

[5] M. O. Gallyamov, I. V. Yaminsky. Nucleic acids, Scanning Probe Microscopy of Biopolymers, A series: Scanning Probe Microscopy. Edited by Prof. I. V. Yaminsky. Moscow: Scientific World, 1 (1997) 25–40. (in Russian).

NONTRADITIONAL METHODICS OF ELLIPSOMETRY

I.E. Skaletskaya

E-mail: skaliron@gmail.com
Telecommunication academy named after Budienny, St. Petersburg, Russia

ABSTRACT

Ellipsometry is a highly sensitive method for studying the surface, its optical properties, and the thicknesses of its surface layers. This is a very promising technique in nanotechnology. This method in the traditional consideration has a number of contradictions in the interpretation of the results. Such notraditional methodics of ellipsometry are highly demanded in nanomaterials science.

Keywords: ellipsometry, polarized optics, main equation of ellipsometry, Fresnel's coefficients.

INTRODUCTION

Nanotechnologies are actively developing and occupy the leading position in the modern world: in science, technology, and technology. For the control of optic properties of nanoobjects (layers, films) the most acceptable and extremely sensitive turn out to be polarized-optic technologies, in particular the ellipsometry.

METHOD

Ellipsometry – is the chapter of optics studying polarization characteristics of light after interaction with substance. This unique method of determining of the optic parameters of materials (N = n – ik): n – the index of refraction, k – the index of extinction, d – the thickness of the films with help of amplitude-phase characteristics of the state of the polarization of the field of reflected wave (ψ, Δ). The method is much more sensitive than energetic method of researches. But this method has a range of internal contradictions connected with the high sensitivity of the decisions of direct task (determining ψ, Δ) and lack of fit of determination of optical parameters of materials (n, k) (the decisions of inverse task).

The main problems of ellipsometry are: angular dependence of optical parameters (n, k) of materials and overstate values of the imaginary part of complex index of refraction compared with habitual values of dispersing absorption.

The key technique is based on using the main equation of ellipsometry (1):

$$tg(\Psi)\exp\{i\Delta\} = R^p/R^s = (E_{refl}^{(p)}/E_{inc}^{(p)})/(E_{refl}^{(s)}/E_{inc}^{(s)}) \quad (1),$$

where R^p, R^s – the integrated Fresnel's coefficients, $E_{refl}^{(p, s)}$, $E_{inc}^{(p, s)}$ – reflected and incident components of radiation for *p* and *s* components, respectively. The analysis was done with help of computer modeling. The problem of non-equivalence and nonequivalence of direct and inverse conformal transformation of nonlinear complex main equation of ellipsometry in analytical model it's decisions for ideal Fresnel's borders is proved rigorously mathematically [1].

EXPERIMENTAL SECTION

The first methodical recommendation: realization multi angles measuring by "0"-scheme of crossed polarizes, especially in surroundings of Brewster's angle and sliding incident angles. In ideal variant is offered construction of device with hole angle access to objects (from 0^0 to 90^0).

The second methodical recommendation for *k* determination: in wide range of extinction values the analytically proved true property (for determine real index of refraction) of invariants of fraction amplitude function to value of material's extinction on Brewster's angle was discovered. These invariants logically named Fresnel's – Brewster's invariants.

To decide the second problem: overstate values of extinction for materials – we propose using the method of measuring of "anomalous reflection". Overstate values of material's extinctions are observed for dielectrics. Semi-conductors show appropriate values of *k* (extinctions). Traditionally in theory *k* is consider only as dispersing absorption. The new point of view is understanding *k* as two-components value (dispersing absorption and radiation scattering). Contribution of scattering and rate of optical roughness of objects is supposed to estimate by values of "anomalous reflection" in angles scanning – the technology of spectroellipsometry [2].

So, angle dependence of optical parameter extinction should consider as mathematically proved and valid fact with interpretation by R. W. Pohl of mechanism light scattering on interface in undersurface structures of materials.

CONCLUSION

In this paper is proposed new techniques to decide problems of traditional ellipsometry.

REFERENCES

[1] Introduction to applied ellipsometry [text]: textbook / E.K. Skaletskiyi [and others] – SPb: IFMO, 2005. – 196 p. (in Russian)

[2] Skaletskaya I.E. Methods and means of polarization-optical diagnostics in nanomaterials science [text]: thesis abstract – SPb: IFMO, 2008. – 27 p. (in Russian)

SECTION 2 :

PREPARATION METHODS AND PROPERTIES MODIFICATION

SELECTION OF OPTIMAL CONDITIONS FOR THE SYNTHESIS OF VANADIUM-TITANIUM CONTAINING NANOSTRUCTURES ON SILICA SURFACE WITH USE OF QUANTUM CHEMISTRY

Drozdov E.O.*, Dubrovenskii S.D.

E-mail: xdeox88@gmail.com
Department of Chemical Nanotechnology and Materials of Electronic Equipment, Saint-Petersburg State Institute of Technology, Saint-Petersburg, Russia

ABSTRACT

A synthesis process of a two-component vanadium-titanium containing monolayer nanocoatings on the silica surface by treating the latter with a mixture of $TiCl_4$ and $VOCl_3$ vapors was considered. Quantum chemical calculations and experimental execution of synthesis have shown that the synthesis temperature and concentrations of the reactants in the gas phase have a decisive influence on the composition and structure of the produced coatings.

Keywords: silica; surface; vanadium oxide; titanium oxide; two-component nanolayer; quantum chemical modeling.

INTRODUCTION

Two-component coatings on silica surface containing vanadium and titanium oxide nanostructures are perspective catalysts in a number of mild oxidation reactions. Monolayer V-Ti systems are of particular interest because of higher efficiency and selectivity [1] and can be synthesized with use of nanotechnological approaches, in particular, by atomic layer deposition (ALD) [2] treating the silica surface with mixture of $VOCl_3$ and $TiCl_4$ vapors.

The purpose of the study was the estimation of the influence of temperature and gas phase reagent concentrations ratio on the composition and structure of vanadium-titanium containing nanostructures on silica surface using quantum chemical approaches and execution of the synthesis in selected conditions.

METHOD

Quantum chemical calculations were carried out by using the Gaussian®09 software package at B3LYP/6-31G(d,p) level of theory [3]. Hydroxyl species of silica surface were represented by cluster model of minimal size (H_3SiOH) using hydrogen atoms as

pseudoatoms [3]. Cluster models of vanadium and titanium containing structures with the number of Si-O-M (M = V, Ti) bonds (denticity, functionality) varying from 1 to 3 were calculated:

Thermodynamic prognosis of equilibrium composition of two-component coatings formed during chemisorption phase was carried out by minimization of total Gibbs energy of the system.

The experimental synthesis of two-component coatings was carried out using ALD method at 200 ^{o}C in gaseous flow of $VOCl_3$ and $TiCl_4$ and dried air as carrier gas. A mixture of gas-phase reagents was obtained by evaporating a mixture of liquid chlorides in a flow of dried air, with a volume ratio of $VOCl_3$ and $TiCl_4$ set in accordance with the results of the calculations.

EXPERIMENTAL SECTION

The calculation results show that the optimum temperature vanadium-titanium containing coating on silica surface is an area of 200 °C, where the ratio of reagents is the main controlling factor. Ratio of vanadium to titanium concentrations in the solid phase $[V]/[Ti]_{solid}$ around 0.5 can be obtained if the ratio of reactants in the gas phase $[V]/[Ti]_{gas}$ is set in range of 8-15.

By varying this ratio, coatings were synthesized with a value of $[V]/[Ti]_{solid}$ from 0.21 to 0.96. The obtained data corresponds to the results of quantum chemical modeling. Based on the calculated vibrational characteristics of vanadium and titanium containing structures, the polyfunctional centers of both modifiers were identified in the diffuse reflectance IR spectra.

CONCLUSION

The study shows the efficiency of using quantum-chemical modeling for solving technological problems of synthesis and spectral identification of multicomponent element-oxide structures, as well as the possibility of using the proposed method for the synthesis of two-component nanoscale coatings.

This study was financially supported by the Ministry of Education and Science of the Russian Federation (grant no. 16.1798.2017/4.6).

REFERENCES

[1] Wachs I.E. Recent conceptual advances in the catalysis science of mixed metal oxide catalytic materials // Catal. Today. 100 (2005) No. 1-2, P. 79-94.

[2] Malygin, A.A. Synthesis of multicomponent oxide low-dimensional systems on the surface of porous silicon dioxide using the molecular layering method // Russ. J. Gen. Chem. 72 (2002) No. 4, P. 575-589.

[3] Malygin A.A., Dubrovenskiy S.D. Quantum-chemical approaches to identification of nanostructures synthesized by molecular layering technique // Russ. J. Gen. Chem. 80 (2010) No. 3, P. 643-657.

RESEARCH OF DEGREE OF SUBCOOLING EFFECT IN THE MASTER ALLOYS ALCR15 CASTING ALLOCATION ISOLATION OF HARDLY SOLUBLE INTERMETALLIDE PHASES AL_4CR AND $AL_{11}CR_2$

Ibragimov V.E., Bazhin V.Yu.

E-mail: ibragimov.vlad@yandex.ru
Department of Metallurgy, Saint-Petersburg Mining University, Saint-Petersburg, Russian Federation

ABSTRACT

Currently, the aluminum industry continues to face various challenges from the use of new nanomaterials. Alloy manufacturers are changing the requirements to improve the quality and cost of aluminum products. The use of master alloys for alloys is constantly changing because of casting technology innovation and market demands alloys. The paper deals with the problem of the influence of the degree of subcooling in the AlCr15 ligature production on the dissolution of the ligature in aluminum alloys.

Keywords: master alloys; intermetallic compounds; aluminum alloys; degree of subcooling

INTRODUCTION

AlCr15 (Cr 15%) master alloy is an effective preparation for alloying aluminum-based alloys with chromium. However, there is a problem of qualitative dissolution of these master alloys in aluminum alloys, which is associated, as practice shows, with the degree of subcooling in the production of master alloys[1]. To analyze this problem, studies have been conducted to identify patterns of precipitation of insoluble intermetallic phases. Master alloy melting with different degrees of subcooling was performed for the analysis.

METHOD

At first, the melting was conducted with a low degree of subcooling with casting in heated corundum molds. Then the bottoms were cast in molds with high degree of subcooling (cast iron casting with heat sink). Resistance furnaces were used to heat and melt the metal. The basis for the ligature was an alloy A8. Chrome was added in the form of cut chips. Melting was carried out in an open atmosphere with the addition of a coating flux.

EXPERIMENTAL SECTION

In the macrostructure of the molten (with a low degree of subcooling) sample, a large amount of gas and shrinkage porosity was found, which is located in clusters in the center and separately in the cross section (figure 1, b). The size of individual pores reaches 0.35 mm. the study of the macrostructure revealed dark inclusions up to 0.14 mm in size, which are rough oxide foams.

During the melting with an insufficient degree of subcooling is present in the ligature in the form of intermetallic compounds Al_7Cr, Al_4Cr и $Al_{11}Cr_2$, the presence of two intermetallic compounds, desirable as these phases at normal operating temperature ligation of the melt, are insoluble.

Chromium intermetallic compounds in the test sample are relatively evenly and densely distributed over the cross section, have different morphology of needles and plates. The volume fraction of intermetallic particles in the ingot is more than 40%. The size of intermetallic compounds varies in the range from 200*100 μm to 1300*150 μm (table 1). The characteristic microstructure of the castings is shown in figure 1.Melting and analysis of the sample with an increased degree of supercooling during casting was also performed (table 2). Here chromium is present predominantly in the phase Al_7Cr.

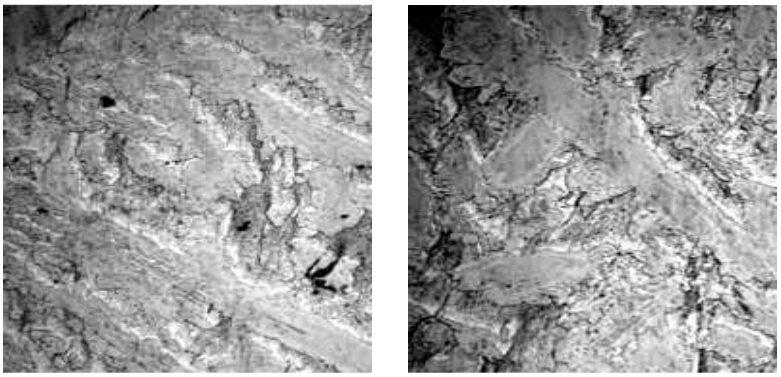

a b

Figure 1. Microstructure pig AlCr15 (Cr-15%).
a - magnification x 100, b - magnification x 200

Table 1. Results of evaluation of the structural components of the sample with a low degree of subcooling (pouring into heated corundum molds)

Volume of fase Al_7Cr, %	Plates and needles Al_7Cr, mkm	Morphology and location Al_7Cr

40	900*300, 300*300, 1100*300,500*500,200*300, 200*900, 1300*150, 1200*100,1100*200	Fragmented irregularly shaped plates and needles, relatively evenly over the cross section

Table 2. The results of evaluation of the structural components of the sample with the high degree of subcooling, greater than 3 times (casting in chilled cast iron molds).

Volume of fase Al_7Cr, %	Plates and needles Al_7Cr, mkm	Morphology and location Al_7Cr
70	700*200, 200*200, 800*200,300*300,100*200, 100*400, 600*100, 600*50,500*100	Fragmented irregularly shaped plates and needles, relatively evenly over the cross section

CONCLUSION

Master alloy with chromium content in the region of 15% during casting with direct contact with the atmosphere, without the operation of gas refining and refining of non-metallic inclusions cannot have good casting properties, the lack of gas porosity. The content of chromium in casting alloys is limited to 0.3% due to the formation of rough forms of intermetallic compounds[2].

In order to avoid high-temperature intermetallic phases such as Al_4Cr, $Al_{11}Cr_2$, the casting of the AlCr15 (Cr-15%) master alloy should occur at a temperature about 980°C with a high degree of subcooling, which is planned to be studied in detail, with an expanded number of experiments in the following works.

REFERENCES

[1] Okamoto, H. (2008). Al-Cr (Aluminum-Chromium). Journal of Phase Equilibria and Diffusion. 29(1), 109. DOI: 10.1007/s11669-007-9225-4.

[2] L. Zhao, Y. Pan, H. Liao, and Q. Wang, "Degassing of aluminum alloys during re-melting," Mater. Lett., vol. 66, no. 1, p, 2012.

APPLICATION OF THIN-LAYER POLYMERIC COATINGS AND FULLEREN C60 TO IMPROVE WEAR RESISTANCE BEARINGS SLIDE

Viktor A. Krasnyy*, Vyacheslav V. Maksarov

*vikras1955@yandex.ru
Saint Petersburg Mining University, Russia

ABSTRACT

It has been shown that bearings of internal combustion engines with an anti-friction layer of lead bronze on the working surface have sufficiently high anti-friction properties, however, in conditions of insufficient lubrication, in the event of an emergency, they are prone to tearing. A technique has been developed for conducting an experiment on a standard friction machine with three modes of lubrication: in conditions of abundant lubrication, when working on lubricant residues at the termination of forced lubrication and without lubricant supply after a long stop. In all cases, a thin polymer coating (3 ... 5 microns) provided a positive effect, especially with limited lubrication and the possible occurrence of scoring.

The tribological properties of fullerene C_{60} were studied and the promise of its use as a coating, as well as in the form of additives to lubricating oils, was shown. The results of studies of fullerene C_{60} as a material that prevents fretting wear during sliding friction of steel and brass samples are presented.

Keywords: wear resistance, polymer coating, anti-friction properties, fullerene C_{60}, fretting wear.

GOALS

The aim of the work was to study the possibility of using thin polymer coatings for additional protection of the working surface of sliding bearings in conditions of insufficient lubrication or in its absence, as well as fullerene C_{60} in the form of a coating and lubricant oil additive to protect surfaces during sliding friction under fretting conditions.

INTRODUCTION

Bearing inserts are essential elements of critical components, the durability of which largely determines the performance and reliability of internal combustion engines. Inserts with antifriction layer of lead bronze on the working surface have high antifriction properties and long-term performance under conditions of normal lubrication, including with high contact loads. However, in the event of emergency situations (termination of lubrication of working surfaces in case of damages in lubrication systems or during forced engine starts without the possibility of preliminary pumping of the lubrication system),

there are tears in both the liners and the contacting parts. For such situations, additional protection can be created by applying thin-layer polymer coatings that act as solid lubricants.

In a number of works, the promise of fullerene C_{60}, fullerene soot and other carbon materials on the boundary sliding friction of metals is noted. A special form of destruction of solids during sliding friction is wear under fretting corrosion conditions. Fretting is characteristic of nominally fixed joints of structures (for example, in places of fastening parts, etc.) and occurs, as a rule, during vibrations leading to various kinds of oscillatory relative displacements and deformations. In some cases, the effectiveness of reducing fretting wear is associated with the use of thin coatings that are sensitive to shear and do not violate the maintainability of machine components. This determines the possibility of using fullerene C_{60} in solving this problem.

MATERIALS AND METHODS

Comparative tests of samples with thin polymer coatings were carried out on a standard friction machine according to the roller-liner scheme with three lubrication modes: I - working under conditions of abundant lubrication (the roller was immersed in an oil bath of 2 mm); II - work on the grease residues after the cessation of lubrication (removal of the oil bath) and a short (5-7 minutes) stop for the oil to run off the roller; III - work after a long parking (20-30 hours) without lubrication.

Fretting-wear samples were tested on a special installation operating on a standard friction machine drive. The effect of fullerene C_{60} on fretting wear of steel and brass samples with steel counterparts was added when fullerene C_{60} was added to the liquid and grease in the form of a powder with a content of 2.5% with intensive mechanical stirring, as well as a coating of a brass sample. The test conditions were as follows: the oscillation amplitude was 150 μm, the frequency was 500 cycles / min, the normal load when tested with lubricant was 4.2 MPa, without lubricant 3.2 MPa.

RESULTS AND DISCUSSION

The test results of the samples showed that the application of a polymer coating on the surface of lead bronze reduced the size of wear spots by an average of 8 ... 10%, and on the surface with an additional tin-lead coating - by 12 ... 15%; reduction of friction coefficient averaged 6 ... 9%. Under working conditions on lubricant residues, the positive effect of the polymer coating increases - applying it to the working surface of the lead

bronze liner reduces the wear spot area by an average of 30 ... 35%, on the tin-lead layer - by 25 ... 30%. At the same time, the friction coefficient decreased by 5 ... 8%. In the most severe test mode (without lubrication under a load of 1000 N), applying a polymer coating to the samples led to a decrease in the area of wear spots by an average of 20 ... 30%.

The test results of fullerene C_{60} for steel samples and contra-samples and for brass samples and steel contra-samples showed that the introduction of powder (2.5%) into the composition of liquid lubricant significantly reduces fretting wear. The wear of the brass specimen with fullerene C_{60} coating was 3 times less than the wear of the uncoated specimen in the absence of lubricant; there was no transfer of copper to the counter sample.

CONCLUSION

The test results of samples with a thin polymer coating showed that such a coating can be used for the working surfaces of the liners of high-loaded bearings of internal combustion engines in order to increase antifriction properties, especially with limited lubrication and the possible occurrence of scuffing.

As a result of the studies performed, the possibility of using C_{60} as additives to lubricating oils, as well as coatings under fretting corrosion conditions for steel and brass surfaces was shown. The data obtained allow us to expand the fields of application of fullerenes for solving complex tribological problems.

REFERENCES

[1] Maksarov V.V., Krasnyy V.A. The mechanisms of friction of thin-layer nano-coatings under conditions of fretting - Scientific and technical lists of the St. Petersburg State Polytechnic University.226, (2015),№3, pp. 111-120.

[2] Krasnyy V., Maksarov V., Olt J. Improving fretting resistance of heavily loaded friction machine parts using a modified polymer composition - Agronomy Research. 2016, 14(S1), pp. 1023-1033.

[3] Krasnyy V., Maksarov V. Specific features of friction mechanisms of thin-film coatings of parts of mining machines working in fretting corrosion - AER-Advances in Engineering Research. 2017, vol. 133 (Actual Issues of Mechanical Engineering AIME-2017), pp. 445-451.

THE USE OF IMAGE ANALYSIS TO STUDY THE MORPHOLOGY STUDY OF POROUS ANODIC ALUMINA FILMS

N.V. Lushpa[1], Dinh Huu Tai[1], K.V. Chernyakova[1], I.A. Vrublevsky[1], E.N. Muratova[2*], Yu.M. Spivak[2], V.A. Moshnikov[2]

E-mail: SokolovaEkNik@yandex.ru
[1]Department of micro- and nanoelectronics, BSUIR, Minsk, Belarus
[2]Department of micro- and nanoelectronics, SPbETU «LETI», Saint Petersburg, Russia

ABSTRACT

Aluminum films approximately 100 nm thick were deposited on silicon substrates (SiO_2 / Si) by thermal evaporation in a vacuum. Porous anodic alumina films were obtained in a potentiostatic mode at 20 V in 0.3 M aqueous solution of oxalic acid and 1.8 M aqueous solution of sulfuric acid. The main pore diameter was determined using the ImageJ software from SEM images. For that an algorithm determining the pore diameter in porous anodic alumina films was developed. It is shown that for nanoporous alumina films formed in sulfuric acid at 20 V, the average pore diameter was 12.3 nm. In the case of the oxalic acid electrolyte the nanoporous alumina films formed at 20 V had an average pore diameter of 14.8 nm. The obtained results are in a good agreement with the literature.

Keywords: anodic alumina; surface morphology; pore diameter; SEM images.

INTRODUCTION

The study of the properties of porous anodic aluminum oxide (AOA) is of great interest because of its unique properties, primarily, such as a highly ordered porous structure, nanosized pores, and the ability to control structural parameters at the stage of their formation using aluminum anodizing [1, 2]. High mechanical hardness, thermal and chemical resistance allows to use anodic alumina for chemical and biochemical separation (filtration), as well as for the synthesis of various nanomaterials, such as nanowires and nanotubes. To expand the areas of application of anodic alumina films and increase the reproducibility of their properties, it is necessary to know the parameters of nanostructure obtained in various modes of anodizing aluminum. It is well known, that the basic properties of anodic aluminum oxide depend on the pore diameter, so there is a need for precise regulation of their geometric dimensions in the process of its formation. In this regard, it is important to apply statistical analysis methods to process large arrays of

nanosized pores and develop a methodology and algorithm to study the surface morphology and nanoporous structure of anodic films [3,4].

METHOD

Aluminum films approximately 100 nm thick were deposited on silicon substrates (SiO_2 / Si) by thermal evaporation in a vacuum. Then, square samples of 4 cm^2 were cut and anodized in a potentiostatic mode at 20 V in an aqueous solution of 0.3 M oxalic acid and 1.8 M aqueous solution of sulfuric acid. The anodizing area of aluminum (about 0.22 cm^2) was set with Viton-o-ring. The process was carried out in a two-electrode fluoroplastic cell at a constant temperature 18 ˚C using a thermostat F 12 (Julabo). As DC power source PS-2403D (Voltcraft) was used. The cathode was a platinum grid. The electrolyte was vigorously stirred using a mechanical stirrer. The main pore diameter was calculated from the SEM images using the ImageJ software.

EXPERIMENTAL SECTION

For processing of SEM images of the of nanoporous anodic alumina surfaces, the ImageJ software was used. Such a program includes all the necessary functions for digital image processing: correction of brightness and contrast, selection of image limits, high-frequency and low-frequency filtering, etc.

The ImageJ software allows us to calculate the areas and statistical values of the pixel values of the various areas selected manually or by means of threshold functions on the images. It supports standard image processing functions, such as logical and arithmetic operations between images, contrast manipulation, convolution, Fourier analysis, sharpening, smoothing, border detection. The program also allows us to perform various geometric transformations, scaling, rotation and reflection. The ultimate task of image analysis is statistical processing of the results obtained when measuring the characteristics of an object with a porous structure, determining the average values of pore diameters, and also plotting graphs to visualize the analysis process. From the surface images of porous anodic aluminum oxide obtained by SEM, the main pore diameter (d_{pore}) was determined using approximation of the pore size distribution curves by the Gaussian function. According to [5,6], it was assumed that the initial pore size distribution contained both initial small-diameter pores and major pores of larger diameter.

Since only the data on the main pores are of practical importance, and the presence of the initial pores interferes with the analysis, some of the pores with a small diameter were not taken into account when approximating. To this end, only one smaller value was

left to the maximum on the pore size distribution curve. The maximum on the Gaussian curve corresponded to d_{pore}. To obtain correct results, the SEM images were processed at least ten times and a new time was selected each time for comparison. Our results shows that d_{pore} = 12.3 nm for porous alumina films obtained in sulfuric acid and d_{pore} = 14.8 nm for the anodic alumina films obtained in oxalic acid. The parameters of the structure of porous alumina films obtained in our work in sulfuric acid and oxalic acid coincide with the data reported in [7].

CONCLUSIONS

Modern software image processing methods have a full set of functions necessary to obtain information about the surface morphology of the nanoporous films. However, the general picture after processing images of nanoporous structures also contains side shapes that arise from surface defects and scratches that make analysis difficult. Therefore, for processing images of nanoporous structures, algorithms that take into account the patterns of growth of nanoporous films are necessary.

Using the regularities of the growth of anodic oxide films at the analysis of histograms obtained by the distribution of pores over the diameter, it was possible to identify a region of results that relates to the oxide growth and determine the pore diameter of nanoporous structures.

Our results shows that d_{pore} = 12.3 nm for porous alumina films obtained in sulfuric acid at 20 V and d_{pore} = 14.8 nm for the anodic alumina films obtained in oxalic acid at 20V.

REFERENCES

[1] Lee W., Park S-J. Porous anodic aluminum oxide: anodization and templated synthesis of functional nanostructures // Chem. Rev. 2014. 114. P. 7487–7556.

[2] Vrublevsky I., Ispas A., Chernyakova K., Bund A. Effect of continuous magnetic field on the growth mechanism of nanoporous anodic alumina films on different substrates // Journal of Solid State Electrochemistry. 2016. 20. P. 2765–2772.

[3] Lushpa N.V., Dinh H. T. Analysis and digital processing of SEM images of anodic alumina films with nanoporous structure // Proceeding of NDTCS-2017. – Minsk: BSUIR, 2017. P. 185–188.

[4] Lushpa N. V., Dinh H. T., Chernyakova K. V., Vrublevsky I. A. Morphological

analysis of nanoporous structure of anodic alumina films with the help of digital image processing // Materials of the international scientific and technical conference: Modern electrochemical technologies and equipment. – Minsk : BGTU, 2017. P. 126–129.

[5] Baron-Wiecheć A., Burke M. G., Hashimoto T., Liu H., Skeldon P. Thompson G.E., Habazaki H., Ganem J.-J, Vickridge I. C. Tracer study of pore initiation in anodic alumina formed in phosphoric acid // Electrochim. Acta. 2013. 113. P. 302–312.

[6] Spivak Yu. M., Sokolova E. N., Petenko O. S., Travkin P. G. Determination of parameters of porous structure in por-Si and por-Al_2O_3 by computer processing of data from raster and atomic force microscopy // Young Scientist, 2012., №5., P. 1–4.

[7] Aerts T., Dimogerontakis Th., Graeve I. De, Fransaer J., Terryn H. Influence of the anodizing temperature on the porosity and the mechanical properties of the porous anodic oxide film // Surf. Coat. Technol. 2007. 201. P.7310–7317.

ELECTROCRYSTALLIZATION OF NANO-DIMENSIONAL METAL ANISOTROPIC POWDERS

Kulinich V.I[1]., Bublikov E.I[2]., Rybalko V.V[3]*., Lyalko E.S.[1]

*E-mail: nano@rosnou.ru
[1]South Russian State Polytechnic University
[2]Don State Technical University
[3]Russian New University, Moscow, Russia

Abstract

The mechanism of electrocrystallization of metal nanowires in a two-layer bath is considered. The results of electron microscopic studies of the structure and morphology of crystals depending on electrolysis conditions, electrolyte composition and composition of the upper layer of a two-layer bath are presented. A crystallographic model of anisotropic growth, the formation of two-dimensional nuclei on different faces of a crystal is proposed. The optimal range of parameters for the crystallization of nanowires has been established.

Keywords: electrocrystallization of nanowires; electron microscopy; crystal growth.

INTRODUCTION

Nanosized metal powders are used to change the magnetic and mechanical properties of materials as catalysts in the chemical industry [1]. The process of electrocrystallization of metals and alloys from an aqueous solution proceeds during the separation of two phases and represents the atomic filling of crystallographic planes under unbalanced conditions.

METHOD

The metal powders of the isometric system of the nanosized range have been obtained by electrolysis at direct and pulse current in a bilayer multicomponent electrochemical system (BES), which consists of a cathode — an organic layer of surface-active compound (SAC) — and anode —an aqueous solution of win salt [2]. It is possible to change the morphology, size and structure of growing crystals in BES by adjusting the ratio of the layer components and the value of the cathode current density.

EXPERIMENTAL SECTION

At the highest values of electrolyte concentration (C_o) and low current density j of the order of 10^4 A/m^2, crystallization of spherulites occurs in the form of processes growing from one center, the length and shape of which change with varying the specified technological parameters and SAC concentration ($C_п$). As the cathode current density decreases and the $C_o/C_п$ ratio increases, three morphologically different stable anisotropic powder formations occur: dendritic, filamentary and fractal. In all forms there are nanocrystal zones with average sizes of 3-5 nm along the anisotropic axes and of 25-30 nm in cross directions, which are the main nanoelements in the formation of a layer-by-layer granulated structure of particles.

Filamentary growth forms occupy an intermediate position between fractal and dendritic objects, which allows to use an aggregation model limited by diffusion [3] to describe the crystallization processes of nanowires.

For α-Fe fractals, separate pieces are poly-twins of random orientation, and crystallographic anisotropy appears only at branch points along one of the diagonals <110> of the side faces of the unit cell of the isometric system. Three different-sized ribs of a pyramid inclined towards each other are distinguished in the minimum volume: a thickened frame, a less developed lateral branch and a small process of the third direction.

As established by transmission microscopy, the cross dimensions of filamentary particles can vary from dozens to hundreds of nanometers, and the length can vary to several dozens of micrometers [4]. Analysis of extinction contours, electron diffraction pattern reflexes, traces of reverse plates and projections of the whisker axes on different planes of the reciprocal lattice shows that there is a sub-granulatedsingle-block structure with small-angle interunit boundariesin the directions of shape anisotropy. Sub-boundaries are formed by misorientation of nanoelements along filling planes at angles not exceeding 4º.

Sometimes it is possible to observe small deviations of the second-order branches from the general orientation of the lateral processes adjacent to them, which is associated with the azimuth component of the misorientation of the main frame subgrains due to their relative torsion. Such a spiral symmetry relative to the shape anisotropy axis appears when the Fe – Co alloy settles [5], which is explained by the diffusion limitations when the microconditionsare changed in the reaction zone. The growth of nanowires is implemented by layer-by-layer crystallization, but the filling planes in this case turn out to be normal to the corresponding axis of the filament. The analysis shows that there is a certain relationship between overvoltage and FC morphology, which is consistent with the results of N.A. Pangarov [6].

CONCLUSION

The influence of parameters in the presence of SAC on the crystallization of powder particles of various morphology and sizes has been studied. Depending on the ratio of the concentrations of electrolyte and SAC at various current densities, it is possible to obtain fractal-like, dendritic and filamentary particles.

The optimum range of parameters for the crystallization of nanowires has been determined.

A crystal model of anisotropic growth has been proposed thatsupports the theory of the formation of two-dimensional nuclei on different faces of a crystal.

REFERENCES

[1] Polyanskii N.B., SerovYu.M., Gryaznov V.M., Bublikov E.I. Mixtures of ultradispersed powders ofiron end cobalt as catalysts for hydrogenationof carbon oxides. Russian Journal of Physical Chemistry A. 2000. T. 74. № SUPPL. 3.

[2] Bondarenko A.V. Electrocrystallization of metal powders: monograph/ BondarenkoA.V., BublikovE.I., KulinichV.I. and others. – Rostov-on-Don: DSTU, 2013. – 121p.

[3] Witten T. A., Sanders L. N., Phys. Rev. Lett, 1981, v 47, p. 1400.

[4] BublikovE.I., KulinichV.I., SemashkevichR.D. Production of nanosized magnetizable powders .Engineering sciences–from theory to practice. 2017. No.1 (61). P. 46-52.

[5] BublikovE.I., KolomietsV.V., KulinichV.I., Lyalko E.S.Peculiarproperties of nanosized powders of iron-cobaltalloy. News of higher educational institutions. North Caucusus region. Series: Engineering sciences. 2016.No.2 (190). P. 102-106.

[6] Pangarov, Crystalliteorientation during metalplating. Crystalgrowthv.10, M.: "Nauka", 1974, P.71-97.

TECHNOLOGICAL SUPPORT OF ROUGHNESS OF PRECISION SURFACES AT THE NANO-LEVEL BY THE METHOD OF FINISHING MAGNETO-ABRASIVE MACHINING

E.G. Zlotnikov, A.E. Efimov, A.I. Keksin, V.K. Drobotukhin

Emails: zlotnik_evg@mail.ru, efim-aleks-evgen@mail.ru, keksin.a@mail.ru, drobotuchin@gmail.com
Saint Petersburg Mining University

ABSTRACT

The problem of forming a surface nanorelief and a near-surface layer with optimal functional properties is relevant for many tasks in various fields of technology and can be solved by using the method of magnetic-abrasive polishing

Keywords: finishing methods., nanorelief, magnetic abrasive finishing, nanotechnology

GOALS

The aim of this article is to show capabilities of magnetic abrasive finishing in the field of nanotechnology.

INTRODUCTION

The most important problem of engineering technology is to improve the quality of the surface layer of the manufactured product. Special signification in this matter are products with complex surfaces, the manufacturing process of which is complicated by their curvilinear spatial form [3]. The number of multi-profile products include cutting tools, in particular taps. The state of the surface layer of the contact surfaces of the teeth of the tap determines not only the performance of this tool, but also the quality of the lateral sides of the internal threaded profile formed by means of it [3].

MATERIALS AND METHODS

From the theory and practice of mechanical engineering it is known that the formation of a threaded profile is carried out by copying on the product the shape of cutting teeth, the quality characteristics and defects of which are automatically transferred from

the surfaces of the teeth to the surface of the product being manufactured [1]. The decisive role in this process is played by the cutting edge and the zone close to it [3], since it is the most loaded part of the wedge-shaped tooth. This fact is confirmed by the fact that tool failures at enterprises due to edge defects occur in 95% of all cases of failures.

Currently, the cutting edges of the tool after sharpening it is desirable to expose additional finishing [1]. Analysis of existing finishing operations of cutting tools showed that the most effective process for the implementation of such tasks is magnetic abrasive machining (MAM). Magnetic abrasive treatment consists in the fact that the powder ferromagnetic abrasive mass, compacted by the magnetic field energy, has an abrasive effect on the workpiece [2, 3], with the latter giving the movements necessary for processing - rotational, oscillating and returning progressive.

In order to solve this problem to improve the quality of the surface layer of cutting edges of the tool (tap), in the Mechanical department laboratory of machines with CNC (computer numerical control) in St. Petersburg Mining University, experimental studies were carried out on magnetic abrasive finishing (MAF) of complex profile surfaces of cutting tools. The device for MAF was based on a milling machine with CNC, which allows to provide the process of processing with all the necessary working movements.

Machine Taps M16 × 2 made of high-speed steel P6M5 were taken as samples. Used to form a magnetic abrasive powder based on titanium carbide and iron (TiC + Fe) was a magnetic abrasive brush in the workspace of the electromagnetic installation system based on a CNC milling machine.

As a result of experimental studies on magnetic abrasive preparation of taps, it was found that in the studied range of technological factors of the MAM process, the radius of rounding of the cutting edges varies within $\rho = 26 ... 64$ μm, roughness - $Ra = 0.09 ... 0.061$ μm, microhardness - $HV = 766 ... 1505$ kgf / mm^2 [3]. The use of MAM for the preparation of taps allows for a relatively short time ($t = 60 \div 210$ sec.) to remove the previous defective layer and form a new one - hardened, round the cutting edges to the required limits and also reduce the roughness of the contact surfaces of the cutting teeth. As an example, Figure 2 shows images of the contact surfaces of the teeth of the tap before and after magnetic-abrasive machining.

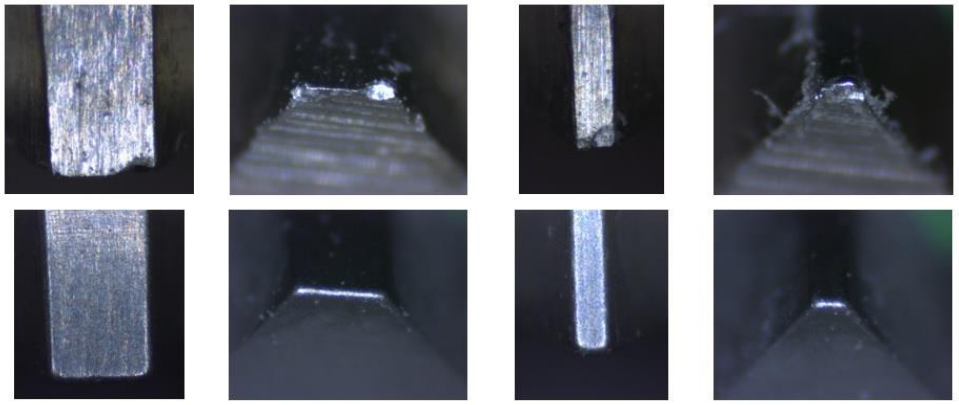

a) b) c) d)

Figure 2. Tap teeth to (top row) and after (bottom row) magnetic abrasive machining: a-b) the 4th tooth in the intake area; c-d) the 6th tooth in the calibration area.

RESULTS AND DISCUSSION

After the preparation of taps with various technological processes of MAM, studies were conducted on cutting internal threads, which took place on a turning-cutting machine tool of the Trens SN 32/750 model under production conditions. Processing was carried out in blanks of corrosion-resistant material (metal thickness 40 mm) brand 08X18H10T. The best result was obtained during magnetic abrasive finishing with powder granularity Δ = 160 μm, magnetic induction B = 0.6 T, polishing time t = 60 s. The parameter of the roughness of the rear surfaces of the cutting edges of the taps was achieved within Ra = 0.061 ... 0.09 μm (61 ... 90 nm) with the initial value Ra = 0.16 ... 0.22 μm [2].

CONCLUSION

In this way, the technology of magnetic-abrasive machining improves the condition of the contact surfaces of the teeth of the cutting tool, which contributes further in the manufacture of the machine-building products with such a tool to improve their quality characteristics and performance properties.

REFERENCES

[1] Khomich N.S. Magnetic-abrasive machining of the manufactured articles. – Minsk: BNTU, 2006. – 218 p. (in Russian).

[2] Olt J. J., Maksarov V. V., Keksin A. I. Internal thread cutting process improvement based on cutting tools treatment by composite powders in a magnetic field / Journal of silicate based and composite materials, №4, Vol. 70, No. 4, 2018. pp. 128-131.

[3] Maksarov V. V., Keksin A. I., Technology of magnetic-abrasive finishing of geometrically-complex products / IOP Conference Series: Materials Science and Engineering, № 4, T 327, 2018. pp.

HETEROGENEITY OF THE THERMOELECTRIC PROPERTIES IN $BI_XSB_{2-X}TE_3$ SOLID SOLUTION PRODUCED BY HOT EXTRUSION

Sergey A. Nemov[a,b], Arseny A. Rulimov[a,*]

*Corresponding author: rulimmmov@gmail.com
[a]**Peter the Great St. Petersburg Polytechnic University, St. Petersburg, 195251 Russia**
[b]**St. Petersburg Electrotechnical University, St. Petersburg, 197376 Russia**

ABSTRACT

During the research we have confirmed and described heterogeneity of the thermoelectric properties in $Bi_xSb_{2-x}Te_3$ solid solution produced by hot extrusion method. This data allows further sorting of pellets cut from extruded material depending on the required values of electrical conductivity and the Seebeck coefficient. Besides the research indicates a number of features in extrusion process for production of such materials.

Keywords: $Bi_xSb_{2-x}Te_3$, thermoelectric materials, hot extrusion, heterogeneity of the thermoelectric properties.

INTRODUCTION

Conversion of heat energy into electrical energy and vice versa using the thermoelectric converters becomes increasingly relevant. These devices possessing a unique combination of design and performance characteristics (like lack of moving parts, noiselessness, autonomy and long service life) have already proven themselves positively both in military-industrial area and everyday life.

One of the main competitive edges in production of the thermoelectric energy converters is production of high-quality thermoelectric materials (hereinafter TEM), particularly by hot extrusion method. Herewith the product of extrusion is often a sample with a circular cross section, from which in turn pellets are cut. This sample is characterized by three parameters (the Seebeck coefficient α, electrical conductivity σ and thermal conductivity χ) included in the thermoelectric efficiency ZT formula:

$$ZT = \frac{\alpha^2 \cdot \sigma}{\chi} T.$$

However, the values of these three parameters are not equal at different points of TEM. Therefore, pellets cut from the same cross section have completely different properties that are not taken into account during production of the converters. There is an attempt to increase efficiency of using extruded pellets by establishing the presence and describing the distribution of the thermoelectric properties in the samples' cross section in this work.

EXPERIMENTAL SECTION

For the study we chose p-type $Bi_xSb_{2-x}Te_3$ solid solution pre-synthesized in an induction furnace. The molar ratio of antimony telluride to bismuth telluride was chosen close to 4:1, because such composition has the maximum value of the thermoelectric efficiency in the solid solution series [1]. Hot extrusion was carried out under an argon atmosphere at a temperature value $T_e > 400^{\circ}C$ and with a moving speed of a punch of 0.3 mm/min.

For the measurements we selected a cylindrical extruded sample with a diameter of 25.4 mm, the Seebeck coefficient value $\alpha = 220$ μV/K and electrical conductivity value $\sigma = 1009$ $(\Omega \cdot cm)^{-1}$. Then we cut 24 parallelepipedal 3.7×3.7×20 mm samples out of it. Such segmentation made it possible to take into account the greater part of the extruded material's cross section. During the processing of experimental data we obtained following heat maps (Figure 1).

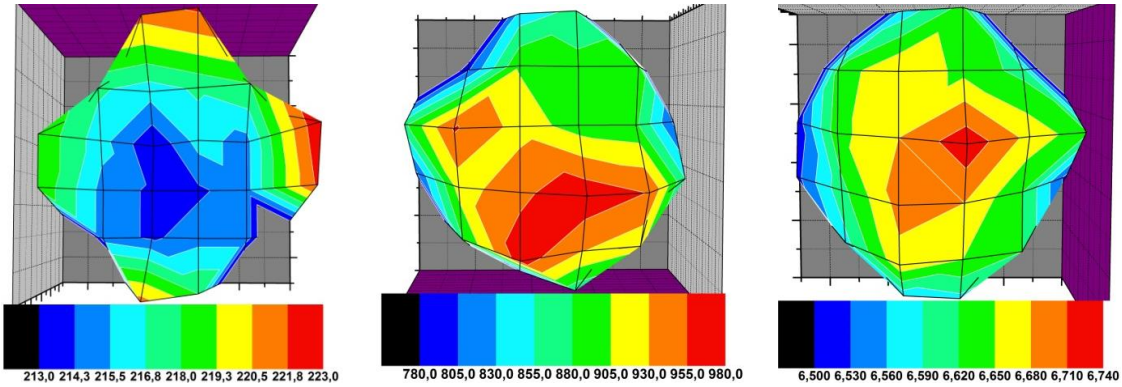

a) b) c)

Figure 1. The distributions of the Seebeck coefficient [μV/K] (a), electrical conductivity $[\Omega \cdot cm]^{-1}$ (b) and density $[g/cm^3]$ (c) in the extruded sample's cross section

Heat maps on Figure 1 clearly indicate the presence of a radial distribution of the properties in the extruded sample's cross section with the maximum of electrical conductivity (Fig. 1b) and density (Fig. 1c) in the central region and the maximum of the Seebeck coefficient (Fig. 1a) in the periphery.

RESULTS AND CONCLUSIONS

Looking at all, the main reason for the above-mentioned heterogeneity of the properties is the heterogeneity of deformation during extrusion process, specifically the presence of large shear deformation of the peripheral regions and its absence in the central zone. Such differences of the stress-strain states were established and described using mathematical modeling of hot extrusion process of the thermoelectric materials, e.g. in [2]. Pyramidal dislocation slip taking place in the peripheral regions under these conditions causes so-called "donor effect" - an increase of electron concentration in the hole semiconductors's conduction band as a result of plastic deformation at high temperatures with low speeds [3]. In practice this effect results in a decrease of electrical conductivity. At the same time such shear deformation has a positive effect on the Seebeck coefficient, while the central zone being less deformed, denser and with fewer defects is characterized by the maximum of electrical conductivity.

The above-mentioned data allows further sorting of pellets cut from extruded material depending on the required values of electrical conductivity and the Seebeck coefficient, if it's necessary. Besides the research indicates a number of features in extrusion process for the production of such materials.

REFERENCES

[1] Keshavarz M.K., Vasilevskiy D., Masut R.A., and Turenne S. p-Type Bismuth Telluride-Based Composite Thermoelectric Materials Produced by Mechanical Alloying and Hot Extrusion // Journal of Electronic Materials // DOI: 10.1007/s11664-012-2284-2. 2012.

[2] Lavrentiev M.G., Mezhenny M.V., Osvensky V.B., Prostomolotov A.I. Mathematical modeling of extrusion process of the thermoelectric materials // Modeling of processes and materials // Materials of electronic technology. Number 3. 2012. P. 35-40.

[3] Gorelik S.S., Ablamsky V.L. In "Structure and properties of the thermoelectric materials" compilation // MISIS, Moscow. 1974. P. 95-99.

SECTION 3 :

FUNCTIONAL PROPERTIES AND PRACTICAL APPLICATIONS

THERMAL FLOWS IN A PCB FROM ALUMINUM WITH ALUMINA OXIDE GENERATED BY A LINEAR HEAT SOURCE

E. Muratova[1]*, V. Moshnikov[1], I. Vrublevsky[2], K. Chernyakova[2], A. Pyatlitski[3], N. Lushpa[2]

E-mail: Sokolovaeknik@yandex.ru
[1] Department of micro- and nanoelectronics, SPbETU «LETI», St. Petersburg, Russia
[2] Department of micro- and nanoelectronics, BSUIR, Minsk, Belarus
[3]«Integral» joint stock company, Kazintsa Str., 121 A, 220108, Minsk, Belarus

ABSTRACT

The paper presents the results of study heat fluxes in a plate made of aluminum with nanoporous aluminum oxide generated by a linear heat source. A carbon filament was used as heating element. It was established that the heat distribution had the form of a heat pipe cone with a beginning from a heat source on the board surface with expansion towards the opposite side. This effect leads to a decrease in thermal resistance of the printed circuit board.

Keywords: nanoporous aluminum oxide, thermal fluxes, thermogram

INTRODUCTION

As known, one of the most important tasks in LED systems is to provide optimal conditions for removing heat from the p-n junction of the die. When the LED is in operation, no more than 25% of consumed energy is converted into light energy, and the rest of the energy is spent on heat loss. Therefore, to ensure high quantum efficiency in LED technology, it is necessary to use effective solutions to remove heat from the working area for the LEDs placement. One of these solutions is use of aluminum printed circuit board with high thermal conductivity [1-3]. The efficiency of heat removal depends on the thermal resistance of the multilayer structure of the metal board. The lower the thermal resistance of the heat sink layers, the better the heat sink. However, in real conditions, the heat distribution on the board with electronic components is not uniform. Therefore, for optimal use of aluminum boards in LED technology, it is necessary to know the real form of heat fluxes in the board volume, which are generated by semiconductor crystals on its surface.

This paper presents the results of study distribution of heat fluxes in the volume of the board made of aluminum with nanoporous aluminum oxide using thermal imaging measurements.

METHOD

In study the samples from aluminum with nanoporous alumina oxide, on the surface of which a linear heating element (carbon conductive filament based on a viscose technical filament) was placed, to simulate an instantaneous linear heat source were used. Samples had the dimensions of 60x24 mm. The thickness of the aluminum base was 0.5 mm. The layer of nanoporous aluminum oxide formed by anodizing aluminum, had a thickness of 20 μm. The carbon fiber with the dimensions of 170x4x0.08 mm was used. The ends of the carbon filament were metallized with a copper (30 μm thick, galvanic deposition) for subsequent soldering of flexible supply electrodes. The carbon fiber filament heater had an electrical resistance of 60 Ohms. To obtain thermograms of the front and back sides of the board, the MobIR M4 thermal imaging camera was used. The data obtained on the temperature distribution on the board surface with the center at the location of the heat source were used to determine the propagation velocity of the heat flow in the board volume in the direction perpendicular to the length of the linear heater.

EXPERIMENTAL SECTION

The thermograms obtained showed that the temperature of the heating element by 5 s of heating was approximately 6.5 °C higher than the temperature of anodic aluminum oxide on the surface of the board. The average temperature of the board increased to 23.3 °C compared to 20.6 °C before the start of heating.

This result indicates the presence of a good thermal contact between the carbon heating element and the surface of anodic alumina for aluminum plate. In addition, it was found that the temperatures on the board surface at the location of the heating element and on its back side at the same point had very close values at all stages of heating. Consequently, the generated heat, due to the high thermal conductivity of aluminum, managed to dissipate over the entire volume of aluminum, providing a uniform profile of temperature distribution over the surface, both on the top and back side of the board.

To determine the rate of propagation of heat fluxes in the volume of aluminum board on thermograms, the distance from the point of heating to the location of the heat front with a temperature of 40.0 °C on the top and back side of the board was measured for 15 s and 20 s from the start of heating.

CONCLUSION

It was found that for a printed circuit board made of aluminum with a layer of nanoporous anodic aluminum oxide in the direction perpendicular to the length of the linear heater, the shape of the heat pipe cone starting from the heating point on its surface was characterized by expansion to the opposite side, which leads to a decrease in thermal resistance. Despite one-sided heating of the aluminum board using a linear carbon heating element, the temperature distribution profile on the back side had a uniform appearance at all stages of heating.

ACKNOWLEDGEMENTS

This work was supported by the Belarusian-Serbian project № F18SRBG-003.

REFERENCES

[1] Muratova E, Moshnikov V, Luchinin V, Bobkova A, Vrublevsky I, Chernyakova K and Terukov E. Thermal-Conductive Boards Based on Aluminum with an Al2O3 Nanostructured Layer for Products of Power Electronics // Technical physics (2018) vol. 63 pp 1626-1628

[2] Vrublevsky I, Chernyakova K, Videkov V and Tuchkovsky A. Improvement of the thermal characteristics of the electric heater in the architecture with aluminum, nanoporous alumina and resistive component of carbon fiber // Nanoscience & Nanotechnology: Nanostructured material, application and innovation transfer (2016) vol. 16 pp 42-432016

[1] Vrublevsky I, Chernyakova K, Videkov V, Tuchkovski A, Dinh T. Utilization of circuit boards on aluminum with nanoporous anodic alumina and copper layer for power modules in switching power supplies // Nanoscience & Nanotechnology: Nanostructured material, application and innovation transfer (2017) vol. 17 pp 40-43.

NANOSTRUCTURED MEMBRANE MF-4SK: POROUS SPACE PARAMETERS AND SORPTION CAPACITY

Lapatin N.A., Borisov A.N., Pak V.N.*

*E-mail: pakviacheslav@mail.ru
Laboratory of surfaces, Herzen state pedagogical university, Saint-Petersburg, Russia

ABSTRACT

Parameters of the porous structure and amount of the active centers has been determined for polymer membrane MF-4SK. Practically, ideal filling of the accessible surface with Zn^{2+} ions is achieved as the result of ion exchange confirming membrane's high sorption

Keywords: membrane MF-4SK; porous structure; sorption capacity

INTRODUCTION

The system of *Nafion* membranes pores is formed in the frame of fluorocarbon and ester chains completed with sulfo-groups at the wall of the internal space. In the absence of the definite knowledge about the internal structure of membranes [1.-3] the presence of pores of different shapes in the range 1-4 nm of conditional diameter is not questioning.

The aim of this work is to define the parameters of the nanostructured pore space and demonstrate high sorption ability of perfluorsulfonic membrane MF-4SK.

EXPERIMENTAL SECTION

Preparation of membranes The analogue of *Nafion* membrane brand MF-4SK was used in the form of thin (0.25 mm) plates with square 1-5 cm^2. Sample sizes were varied according to reliable weight, sorption and optical measurements. Samples were subjected to clean-up by boiling in concentrated nitric acid for 2-3 hours followed by thorough washing with water, then dried at 90^oC and stored in a desiccators over calcined zeolite.

RESULTS AND DISCUSSION

Water adsorption, estimation of specific surface and membrane pore volume were measured at room temperature by the gravimetric method in the range p/p_o = 0.1-0.99

of relative vapor pressure. Figure 1 shows numerical values and weakly pronounced *S*-shaped type of adsorption isotherm. The relevant order of *S* magnitude is of interest. Taking in account the conditional value of adsorbed water monolayer capacity $a_m \approx 0.04$ g/g at p/po = 0.3 (Fig. 1) and the landing area of water molecule ω = 25 Å^2, we come to solid value $S = a_m \cdot \omega \cdot N_A \approx 300$ (m^2/g). The value of the mass increase relative to dry (at 90°C) state, meets the membrane sorption volume $V_p = 0.20 \pm 0.03$ cm3/g based on the results of several measurements.

Sulfogroups content in the membrane [-SO_3H] was determined by the method of reverse titration. Samples dried at 90°C up to constant mass, were immersed in an aqueous solution of NaON on 3-4 hours to ensure full replacement of protons for sodium ions. Then the balance of alkali was titrated with hydrochloric acid (Fig. 2). The value [-SO_3H] was judged by alkali loss in solution as a result of his contact with the membrane sample. According to the results of 5 definitions it was established as [-SO_3H] = 0.84 ± 0.05 mmol/g.

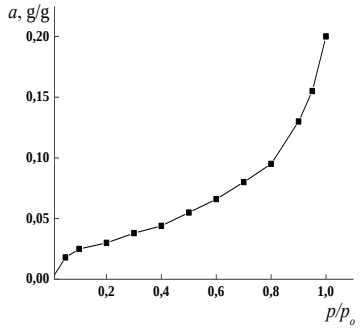

Fig. 1 Isotherm of water adsorption; residual
a - the amount of adsorption, solution
p/p$_0$ - relative vapor pressure membrane

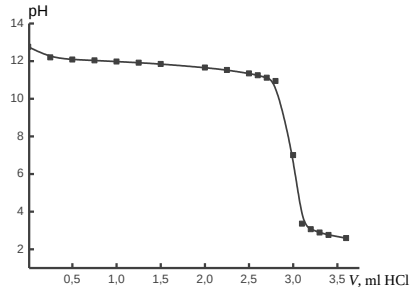

Fig. 2 Titration curve of the alkali after contact of NaOH (20 ml; 0/0192 mol/l) with of 0.1 g by mass (concentration solution is 0.1 mol/l)

of HCl

Ion-exchange membrane capacity

As an example considered by Zn^{2+} ion sorption (membrane dried at 90^0C, mass ~ 0.05 g maintained in 20 ml 0.1 mol/l water solution of $ZnCl_2$). Limit value of sorption of Zn^{2+} is reached within 1 hour and sustainably reproduced at the level of 0.45 ± 0.04 mmol/g in all cases where the full content of ions in solution exceeds the sorption capacity of the membrane.

Fixed form of Zn^{2+} is hydrolytically resistant and completely preserved in the course of repeated washing the membranes from the pore solution. Sorption ratio of Zn^{2+} amount to the content of membrane [-SO_3H]-groups is near ½ allowing to confidently believe that ion exchange flows according to the scheme $2(-SO_3H) + Zn^{2+} \rightarrow (-SO_3-)_2Zn + 2H^+$ and provides the filling limit of the surface with ions.

CONCLUSION

Perfluorsulfonic membrane MF-4SK was characterized as highly efficient sorbent. The top level sorption capacity of the membrane reflects a combination of advanced porous structure with uniformity and dense distribution of high-activity centers -SO3H on the accessible surface.

REFERENCES

[1] Heiter-Wirguin C. Recent advances in perfluorinated ionomer membranes: structure, properties and applications // J. Membr. Sci. 1996. Vol. 120. No 1. P. 1-33

[2] Mauritz K.A., Moore R.B. State of understanding of Nafion // Chem. Rev. 2004. Vol. 104. No 10. P. 4535-4586.

[3] Kristensen M.B., Catalano J., Haldrupa S., Bělský P., Tomáš M., Bentien A. Tuning the ion channel network of perfluorosulfonated membranes via a facile sacrificial porogen approach // J. Membr. Sci. 2018. Vol. 545. P. 275-283.

CONCEPTS OF STUDENTS TRAINING ON "NANOENGINEERING" EDUCATION DIRECTION

Y. V. Panfilov, S. B. Nesterov, Y. B. Tsvetkov

panfilov@bmstu.ru

Department of Electronic Technology in Machinery

MSTU named after Bauman, Moscow, Russia

ABSTRACT

An experience of students training on "Nanoengineering" education direction at the Department of Electronic technology in machinery of MSTU named after Bauman was described. Main significances of education process on "Engineer nanotechnology in machinery" division were emphasized. Professionally orientated students training system based on the "Russian method of engineer training" was presented.

Keywords: nanoengineering; machinery; electronic technology; education.

INTRODUCTION

Educational methodic for any nanotechnology fields should be constructed on the concept of a reasonable combination of classical engineering education with special knowledge obtaining on physical and mathematic disciplines and special chemical disciplines [1].

METHOD

The course of training in engineer nanotechnologies should carry emphasis on the next sections:

1. Entirely new technical decisions search methods. For example, method of severe plastic deformation for obtaining nanostructured materials, or planar technology in microelectronics as a way for changing hybrid integral circuits on monolithic semiconductor circuits;

2. Theory of machine productivity as a "tool" for crucial evaluation of processes and equipment for nano-objects manufacturing from the point of their viability for high production rate output and cost-efficiency;

3. Optimal combinations of nano, micro and macro elements in machines and devices in order to find methods with consideration of self-organization phenomenon and effects under any nanostructures manufacturing;

4. Professionally oriented methodic of students training throughout continuous quarter by quarter students practical work.

Educational program in "Engineering nanotechnology in machinery" includes common engineering disciplines that student should pass mandatory. Among them is such discipline as "Process equipment design", "Mechanism's calculation and design", "Automatic control systems elaboration", "Modern technological and analytic equipment service and renovation" and others are among the most important ones. This is important for us to keep those disciplines in order to maintain the traditions of our designer school.

EXPERIMENTAL SECTION

To realize the first section, wireless electronics with miniature antennas disposed on every chip of nanodimensional circuit instead of contact pads was suggested. Besides this, the real perspective of thin film nanostructures for quantum calculation creation nowadays has appeared.

"History perspective" of nanotechnology deals with offering products to series or mass production, analogously with home electronics or automobile conveyor. So, we think compulsory for education is a number of disciplines related to machine and device production technology, and process and production automation as well [2].

The third section disciplines must be based on some classical subjects, such as technology of machinery. The priority goal is the manufacturability of machines and devices, convenience of their manufacturing and service.

As an example of the implementation of the fourth section, educational discipline "Engineer practical work" [3] was suggested. At the Department of Electronic technology in machinery" of MSTU named after Bauman it goes back to more than 25 years ago. The "Engineer practical work" spreads on three quarters for bachelor students and on four quarters for magister students. This discipline realises two methodical tasks at once: the real individual training of students and the possibility for every student to choose the direction of special training according to his or her inclinations and abilities.

The "Engineer practical work" goal is obtaining by every student engineering skills at laboratory or industrial conditions by the way of students direct participation in decision-making in highly demanded scientific or production problems. Topics of student work are determined in accordance with the scientific or production interests of student's mentor or

R&D division. So, in engineering group of the department or R&D laboratory or manufacturing division, every student is involved as co-executor of current work. As a result of "Engineer practical work" , every student obtains material for final qualification paper.

CONCLUSION

Previous experience of engineering education prompts the necessity of evolutionary development of basic engineer training in the field of machine and device construction in combination with new knowledge obtained in the field of nanotechnology. Professionally oriented students training system based on the "Russian method of engineer training" is designated to help students in obtaining engineering practical experience. This is achieved by educational discipline "Engineer practical work".

REFERENCES

[1] Panfilov Y.V. Direction of students training on "Nanoengineering" at MSTU named after Bauman // Nanoengineering, No. 8, 2014, P. 4 – 6.

[2] Punfilov Y.V. Vacuum technological equipment analysis by criterion of productivity / In book: Productivity and Reliability of Technological Systems in Machinery, 2015, P. 48 – 53.

[3] Kamenikhin A.T., Panfilov Y.V., Tsvetkov Y.B. Engineer practical work // Nanoengineering, No. 8, 2014, P. 37 – 48.

SHORT COMMUNICATIONS TO EDITOR

THERMODYNAMIC MODELING POSSIBILITIES OF PHASE-CHEMICAL TRANSFORMATIONS FOR THE PROCESSING AND SYNTHESIS CONDITIONS OF HIGH-DISPERSED MATERIALS

Slobodov A.A.[1,2], Gorshkova R.M.[3], Yablonsky G.[4], Sochagin A.A.[1,2], Slobodova D.A.[3.5], Ralys R.V.[1], Radin M.A.[5]

[*]E-mail: aslobd@gmail.com

[1]ITMO University
[1]Saint Petersburg State Institute of Technology
[3]Institute of Macromolecular Compounds of the Russian Academy of Sciences
4Saint Louis University (MO, USA)
[5]Saint Petersburg State University of Industrial Technology and Design

Experimental investigation of simultaneous chemical and phase transformations occurring in a variety of chemical processes under the conditions of synthesis of materials with demanded properties is still too difficult in the modern science and technology and therefore has incomplete solution. For many systems and processes the justified and the most efficient way to investigate them is to use thermodynamic modeling, rather than conducting elaborate and expensive experiments to gather the information needed. In principle, thermodynamic modeling has the major advantage of being highly rigorous, and thus, more informative and detailed than direct experiments.

However, efficiency of such an approach, meaning we obtain reliable and quantitatively justified, could be reached only in case if we meet a set of conditions. This set includes: 1) correctness of a system description, including thermodynamic and thermochemical data, which describe both initial substances and possible products; 2) effectiveness of solution applied to the system of interest; 3) adequate interpretation of the results obtained via modeling.

Determination and elaboration of all main aspects of the problems set, their subsequent analysis, and finding a way to a solution all happen when we rigorously consider central and purely thermodynamic problem, i.e. solve the general problem of identifying phase and chemical transitions in an arbitrary multicomponent system.

First, we consider the system consisting of *m* basic or Gibbs components. We assume that these components form *n* species as a result of all chemical reactions possible. The number of all species *n* is not less than the number of components *m.* This number includes species in solid phases, compounds in both neutral and ionic forms, dissolved gases, etc. The difference *n-m* is the number of dependent substances in all forms available, e.g., gases dissolved in liquid solutions, ions, precipitated solids, etc. The total quantity of components across all species in the reacting system always remains same independent of which

transformations take place. This reflects natural constraint imposed on the system and is the so-called material balance condition. This balance states that absolute content of each component in the sum of all species in all phases expressed either in moles or in mass units keeps constant $\{y_j^o\}_{j=1}^m = const$.

The system is in equilibrium when a function characteristic to external conditions is in its global minimum point and satisfies the material balance constraint. In case of constant pressure *P* and temperature *T*, we minimize the total Gibbs energy of the system in the following form:

$$\begin{cases} G = \sum_{i=1}^{n} \mu_i y_i \equiv \sum_{i=1}^{n} \left(\mu_i^0 + RT \ln \gamma_i x_i \right) y_i \to \min\limits_{\{y_i\}} \\ \sum_{i=1}^{n} a_{ij} y_i = y_j^0, \quad j \in 1:m \\ y_i \geq 0, \qquad\qquad i \in 1:n \end{cases} \tag{1}$$

where y_i^0 is the number of moles of basic components of the system; a_{ij} is the stoichiometric matrix of the system; y_i is the number of moles of all species in equilibrated system; μ_i is the chemical potential of the species *i*, μ_i^0 is the standard chemical potential of the species *i*; x_i is the molar fraction of the species *i*; γ_i is the coefficient of activity of the species *i*.

Coefficients of activity depend on the model of excessive functions describing nob-ideality of the system. In systems with pure substances, we should consider conditions where $x_i = \gamma_i = 1$, i.e. $\mu_i = \mu_i^0$ and, thus, phase transitions.

The problem described in system (1) consists of the three major parts:

1) Condition of minimum of the function of *n* variables – the total Gibbs energy;
2) Condition of basic components preservation;
3) Condition of non-negativity of the quantity of any species presented in the system.

In order to illustrate possibilities of the methodology we offer in this work, let us describe a few real life cases, which have drastically different phase and chemical nature. In the fig. one may see how temperature influences the process of ceramics synthesis in the system made of fourteen elements. Phase and chemical transitions shown in this figure give us the justified answers on which phases and in which quantities are formed, how their composition depends on gas composition and properties, which gaseous products are evolving during the synthesis.

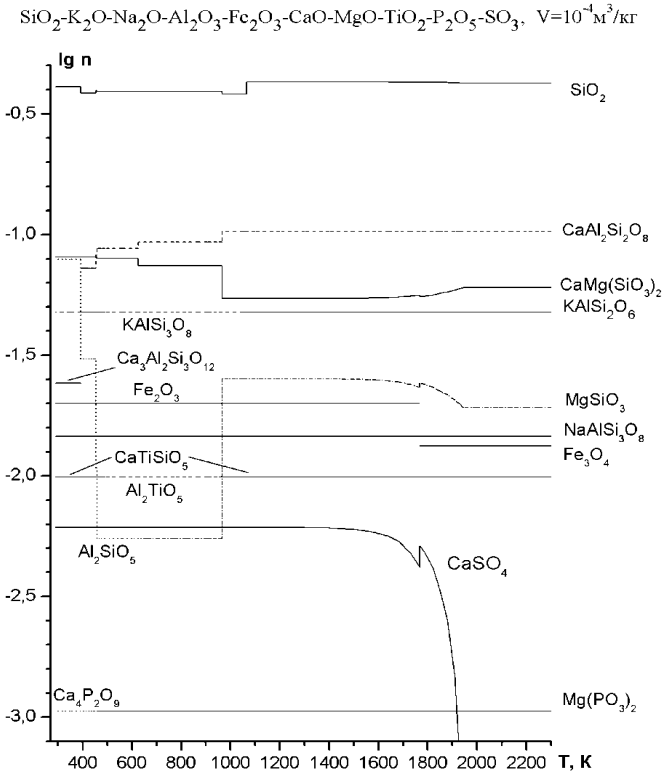

Figure 1.

The data we obtained as a result of modeling and computation with help of our software, not only show good coherence with well known experimental data, which in most cases tend to be scarce and incopmlete, but also provide us with more qualitatively and quantitavely information about mechanisms of processed taking place in the systems of interest.

Bogdanov S. P.[1], Khristyuk N. A[1]., Kozlov V.V[1]., Dolgin A. S.[2]

E-mail: BogdanoSP@mail.ru
[1]St.Petersburg State Institute of Technology (Technical University)
[2]Grebenshikov Institute of Silicate Chemistry, Russian Academy of Sciences

ABSTRACT

The conditions of gas transport of metals Ti, Zr and Mn on corundum powders for obtaining composite materials of core-shell type are studied. The ceramic plates from the clad powders are obtained. The properties of the obtained materials are studied.

Keywords: coatings for powder; gas transport; corundum; core-shell powders.

Due to the combination of high hardness, heat resistance, chemical inertness and availability, aluminum oxide is widely used for the manufacture of technical ceramics. To reduce the sintering temperature, various additions of activators in the form of oxides or salts are introduced into the mixture [1]. Despite the fact that each company uses its own set of activators, the method of their introduction is the same and consists in a long grinding. This technology is simple, but leads to a decrease in the quality of products due to the heterogeneity of their properties. Obviously, for a uniform distribution of the added additions in the composition, the best option is to distribute them as a thin layer on the surface of the grains of the original corundum powder.

In this work, the gas transport method is used to obtain nanolayer activators on the surface of corundum grains. Iodine was used as a transporting agent [2-4]. A new approach to the synthesis of shells on the surface of alumina powders designed for the technology of activated sintering of ceramics has been developed. Both metallic coatings and joint oxide systems were obtained from the Al_2O_3 core and the TiO_2, ZrO_2, $MnAl_2O_4$, $MnTiO_3$ shells and their composition.

The morphology and distribution of chemical elements in clad powders was studied by scanning electron microscopy. It has been established that for full transfer of Ti, Zr, Mn to the surface of corundum in two hours a temperature of 800°C is required. The optimal composition of the mixture and the modes of deposition of nanoshells on the surface of aluminum oxide, intended for ceramics technology are selected.

At the second stage, the modes were selected and the laws of sintering of ceramics based on particles with 'skin-layers were studied. Electron microscopy data in back scattered electrons (Fig. 1) show a significant difference in the nature of the distribution of the activator in the composition between the industrial ceramics sample (Fig. 1a) and the

experimental ones (Fig. 1b). Industrial and experimental samples had an identical set of activators, but differed by the method of their introduction. The industrial design was sintered from a mixed charge, and the prototype was sintered from a clad corundum powder. Figure 1a shows zones containing a large amount of activator (bright white areas) and zones in which the activator is completely absent. In Figure 1b, the activator is evenly distributed in the composition. Enlarging the image and building maps of the distribution of elements shows that the activator is distributed at the boundaries between corundum particles.

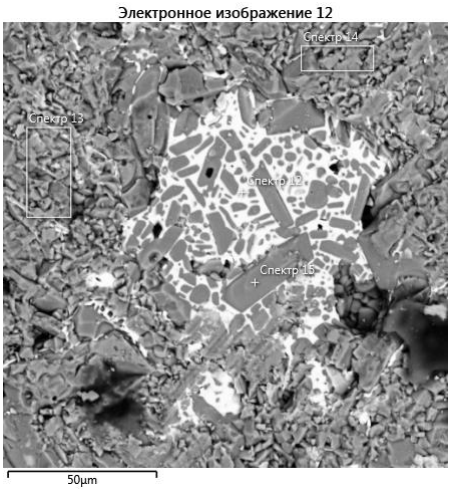

a)

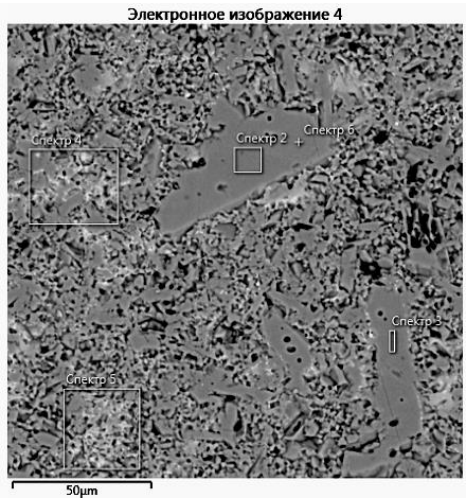

b

Fig 1. SEM-image of corundum ceramics in back - scattered electrons (BSE); a) Industrial design, sintered from the mixture obtained by mixing Al_2O_3 with activators, b) sample, sintered from the mixture obtained by cladding Al_2O_3 by the method of iodine transport.

The phase composition and mechanical properties of ceramics are investigated. The use of Al_2O_3 // ZrO_2 core-shell powders made it possible to obtain a practically non-porous material with a maximum relative density of 99.5%. However, the maximum values of mechanical properties are achieved during sintering of corundum clad with a combined coating consisting of $MnAl_2O_4$ and TiO_2; microhardness up to 22.5 GPa, elastic modulus up to 408 GPa.

The work was financially supported by the Russian Scientific Foundation (project no. 17–13–01382).

REFERENCES

[1] Pavlushkin N.M., Spechennyi korund (Sintered corundum), Moscow: Gos. Izdat. Stroit., Arkhitekt. Stroit. Mater., 1961.

[2] Bogdanov S.P., Preparation of coatings on powders by the iodine transport method, Glass Phys. Chem., 2011, vol. 37, no. 2, pp. 172–178.

[3] Bogdanov S.P., Iodine transport method for production of coatings on powders, Izv. SPbGTI(TU), 2012, No. 16 (42), pp. 24–28.

[4] Bogdanov S. P. Iodide Transport - Method of Synthesis of Inorganic Materials // Smart Nanocomposites. – 2014, v.5, i.1, P.1-8.

PECULIARITIES OF DIFFUSION CHROMIZING OF HIGH CARBON STEEL U-12 BY MEANS OF IODINE TRANSPORT

Khristyuk N. A[1]., Papandreopoulos P[2]., Bogdanov S. P.[1]

E-mail: nikolai.hristyuk@mail.ru
[1]St.Petersburg State Institute of Technology (Technical University)
[2]Athens Polytechnic University

ABSTRACT

The process of diffusional chromizing of steel U -12 was studied. The microstructure, phase composition of coating and their mechanical properties were determined.

Keywords: chromizing, coatings on the steel, iodine transport.

High carbon proeutectoid steels (more than 0.8% C mass) have a high hardness, wear resistance and good strength due to the large the content of the phase Fe_3C (cementite) in their microstructure and are used for manufacturing various cutting tools. However, their corrosive persistence is small. One way to protect against corrosion of products from these materials is diffusion chrome plating. In the previous works of the authors [1] phase and kinetic laws of diffusion chromium plating are established hypo eutectoid steels by iodine transport. The purpose of this study is to determine these dependences for steel grade U - 12 (C content - 1.25% by weight).

The temperature and time parameters of the process were set similarly to [1]. The thickness of the coatings was determined by measuring the transverse microsections on scanning electron microscope (SEM) Tescan Vega 3 SBH with a prefix for x-ray micro X-ray analysis Aztec X - act. Phase composition of coatings studied by X-ray diffraction (XRD) analysis on a Rigaku SmartLab 3 diffractometer. The microhardness of the surface was determined by the device PMT - 3. It was also determined the continuity of the coatings by the fingerprinting method of potassium hexacyanoferrate II solution, reacting only with iron. Thus, discontinuous areas appear as blue spots.

The formation of thin coatings begins at a temperature of 500 ºC, thickness which do not exceed 1 micron. The growth of solid coatings begins with a temperature 700 ºC. As with materials with a lower carbon content described by a parabolic law, reaching 4 microns. (at a temperature of 700 ºC). An increase in temperature causes a further increase in coating thickness: at a temperature of 800 ºC thickness is 6 microns, at a temperature of

900 ºC - 11 microns (with exposure in the oven - 6 hours). According to XRD data, all carbide coatings nature Low-temperature treatment leads to the growth of the $Cr_{23}C_6$ phase.

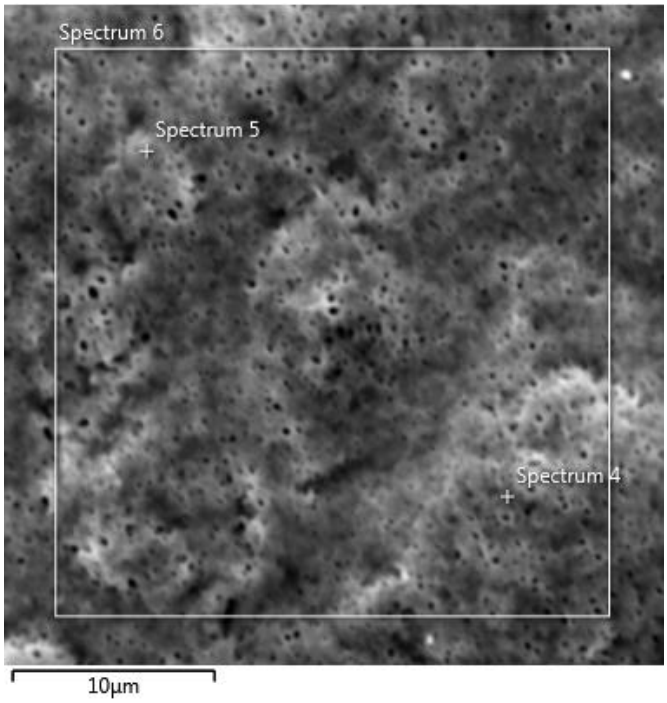

Figure 1. SEM morphology of coating which was obtained in 900ºC per 3 hours.

Beginning with temperatures of 700 ºC, a more chromium-rich carbide, Cr_7C_3, appears which with a further increase in temperature increases. According to morphological characteristics of the coating is an intergrowth of chromium carbide crystallites small size with a small content of Fe: 2 - 3% by weight (figure 1, spectrum 4, 5, 6) and iron content increases slightly with a decrease in the temperature of deposition. Also on all samples, surface porosity with pore size is present. up to 1.5 microns. It should be noted that the porosity is not through - on transverse thin sections the coating is solid. The microhardness of coatings reaches 16 GPa, indicating their high wear resistance combined with good corrosion resistance.

REFERENCES

[1] Bogdanov S. P. Diffusional chrome plating of steel by iodide transport // Steel in translation. – 2017, v 47, № 1, pp. 78 – 83.

IMPROVING THE ACCURACY AND RELIABILITY OF MECHANICAL PROPERTIES MEASUREMENTS OF NANOMATERIALS AND NANOCOATINGS

Gogolinskii K.V. [1*]***, Umanskii A.S.*** [1]***, *Mescheriakov V.V.*** [2]

**nanoscan@yandex.ru*
[1]**Saint-Petersburg Mining University, Saint-Petersburg, Russia**
[2]**MEPhI, Moscow, Russia**

ABSTRACT

The report is devoted to new methodological and technical solutions in the field of mechanical properties measurements of nanostructured materials, thin coatings and other nanoscale objects. The described approaches are based on the method of instrumental indentation.

Keywords: instrumental indentation; mechanical properties; nanomaterials; thin coatings.

For construction nanomaterials, protective and functional nanocoatings, mechanical properties are one of the key quality indicators. Method of instrumental indentation [1] is used for solving this objective mostly often.

The measurement's accuracy of hardness and elastic modulus within the described method is significantly influenced by the following: -the distortion of the indenter geometry on a scale less than 100 nm; - the dependence of the propagation of elastic-plastic deformation in a material on the shape of an indenter [2]. This leads to the deviation in numerical values of hardness and elastic modulus obtained during measurements on the same sample using different machines. In modern metrology, the standard that reproduces the hardness scale is the device (reference machine) and the transfer of hardness scale is carried out using reference test blocks. This approach does not provide proper reproducibility of the measurement results at the nanoscale. Experience shows that the difference in the results of measurements of the same samples on different devices may exceed 15% even during comparisons of national primary standards. At the same time, the random variation of measurements (standard deviation) on the same samples does not exceed 5%. [3]. As a solution to this problem, the authors suggest using reference materials of chemically and mechanically homogeneous materials with known properties to calibrate nanohardness testers. Fused silica, monocrystalline sapphire and polycarbonate are traditionally used as reference materials. This range should be expanded, in particular, by reference materials of metals and their alloys. The authors proposed the method of

individual calibration of the hardness tester by correcting the function of the indenter shape on samples with known properties [4].

An important problem of measuring of the mechanical properties in the nano-range in manufacturing environment is the effect of temperature drifts of the measuring system, convective ambient air flows, mechanical vibrations and electrical noise. The use of sensors for nanohardness testers operating in self-oscillation mode makes it possible to radically expand the possibilities of measurements. A new dynamic method is proposed for measuring the value of local hardness and contact stiffness in the nanoscale range using a probe in the self-oscillation mode at its own resonance frequency [5]. The value of the applied force is measured by the frequency change of self-oscillations. The advantage of the method is the absence of the drift component in the measuring signal during the test cycle.

REFERENCES

1. Oliver W. C., Pharr G. M. J. Mater. Res. 2004. V. 19. N 1. P. 3 – 20.

2. A.C. Fischer-Cripps Introduction to Contact Mechanics, Springer Science+Business Media, LLC, 2007.

3. Aslanyan A., Aslanyan E., Menelao F., Li Z. VNIIFTRI / PTB bilateral comparison on martens and indentation hardness scales, Proceedings: XXI IMEKO World Congress , Prague, Czech Republic 2015. P. 792 –794.

4. Potapov A.I., Gogolinskii K.V., Kondratiev A.V., Umansky A.S. Control. Diagnostics. 2017. No. 2. P. 28-32. (in Russian).

5. Meshcheryakov V.V., Maslennikov V.V., Melekesov E.V. Measurement Techniques. 2017. C. 771-776.

FORECASTING OF THE RESOURCE OF STRUCTURAL MATERIALS BASED ON THE ESTIMATION OF THEIR STRENGTH NANO-CHARACTERISTICS

Nosov V.V.[1, 2], Grigoryev E.V.[1] , Gilyazetdinov E.R.[1], Chaplin I.E.[1]

E-mail: nosovvv@list.ru
[1]**Instrumentation Department, Saint-Petersburg Mining University, St. Petersburg, Russia**
[2]**Peter the Great St.Petersburg Polytechnic University, St. Petersburg, Russia**

ABSTRACT

The principles of selection and methods of evaluation of strength nano-characteristics of representative reference structural elements of the material on the basis of information filtering of the results of registration of acoustic emission signals from the position of the micromechanical model of its parameters.

Keywords: acoustic emission (AE), AE parameter, universal physical nanoconstants

The forecasting of the resource of structural materials and goods made using them is currently based on the connection of the laboratory studies results of the strength of standard macro patterns with the strength characteristics of the material in a real object. The heterogeneity of the strength properties and conditions of control of different zones of the material of a real complex object makes this connection polysemantic, bringing the uncertainty in the results of the control. The solution of the problem is connected with the need of the information transfer to the micro- and nano-level control, which determines the strength, and with the use of representative microstructural elements of the material and universal physical nanoconstants as a model.

The approach to the processing of primary AE information makes it possible to formulate the energy, structural and time-dependent characteristics of strength according to micro- and nano-levels, to propose a number of valuable diagnostic AE parameter of the strength condition (Table 1, [1–8]) based on algorithms for non-destructive AE strength control.

Table 1

Some concentration-kinetic AE parameter of the strength condition of technical objects

that are resistant to the influence of destabilizing factors

where ξ is the primary parameter AE, $A_D = k_{AE} C_0 / \{ \tau_0 \exp[(U_0 - \gamma\sigma(t))/(KT)] \}$, k_{AE} is the acoustically controlled volume of the material, K_H - load factor (the ratio of the diagnostic load to the working load).

Time to destruction at constant load (σ=const)

AE parameter	Micro-model	Nano-model	Characteristic
X_{AE}	dlnξ/dt	$\dot{\gamma}\sigma / KT$	nanostructure
Y_{AE}	dlnξ/dσ	γ / KT	nanostructure
Z_{AE}	lnξ-lnA_D	$\omega = \gamma\sigma / KT$	danger of destruction
ΔZ_{AE}	$\ln\xi_1$ - $\ln\xi_2$	$\omega_1 - \omega_2$	relative danger
F_{AE}	$\ln\xi_1/\ln\xi_2$	σ_1 / σ_2	relative load
W_{AE}	dlnξ/dKн	$\omega = \gamma\sigma / KT$	danger of destruction

$$t^* \approx 10^{-15} \exp(U_0 / KT - Y_{AE}\sigma) = \exp(M - Y_{AE}\sigma) = B / \exp W_{AE},$$

where $M \approx U_0 /(KT) - 34, \quad B = \exp M$

Strength limit

$$\sigma_B \approx M / Y_{AE}$$

Load of destruction

$$F_{рп} = (U_0/(KT)+\ln(\tau_0 C^*/C_0 F_p' \cdot k Y_{AE}))/(k Y_{AE}),$$

where U_0 - activation energy of the process of destruction of the material, K - Boltzmann's constant, T - absolute temperature, τ_0 - period of atomic oscillation, C^*/C_0 is the ratio of the critical C*and C_0 the initial concentration of micro cracks and structural elements, respectively, Fp' is the rate of growth of load when loading, k= σ/F is the coefficient of proportionality between stress σ and the external load F on the specimen.

The number of cycles to destruction

$$N_C = N_B / \exp W_{AE},$$

where N_B – material characteristic parameter, temperature and frequency of loading, determined by the stress-cycle diagram of samples of this material, γ- structural-sensitive coefficient (nano-characteristic of the strength of a representative structural element of the material), $\omega = \gamma\sigma / KT$ - strength condition parameter.

REFERENCES

[1] Nosov V.V. Mekhanika kompozicionnyh materialov. Laboratornye raboty i prakticheskie zanyatiya: Uchebnoe posobie. Saint-Petersburg: Lan', 2013, p. 240

[2] Nosov V.V. Automated Evaluation of the Service Lives of Specimens of Structural Materials on the Basis of a Micromechanical Model of the Time Dependences of Acoustic Emission Parameters//Russian Journal of Nondestructive Testing, 2014, Vol. 50, No. 12, pp. 719–729.

[3] Nosov V.V. , Potapov A. I. Acoustic Emission Testing of the Strength of Metal Structures under Complex Loading //Russian Journal of Nondestructive Testing, 2015, Vol. 51, No. 1, pp. 50–58.

[4] Nosov V.V. Diagnostika mashin i oborudovaniya: Uchebnoe posobie, Saint-Petersburg: Lan', 2016, p. 376

[5] Nosov V. V. On the Principles of Optimizing the Technologies of Acoustic-Emission Strength Control of Industrial Objects// Russian Journal of Nondestructive Testing, 2016, 2016, Vol. 52, No. 7, pp. 386–399.

[6] Nosov V. V., N.A. Zelenskii. Estimating the Strength of Welded Hull Elements of a Submersible Based on the Micromechanical Model of Temporal Dependences of Acoustic-Emission Parameters// Russian Journal of Nondestructive Testing, 2017, Vol. 53, No. 2, pp. 89–95.

[7] Nosov V. V. Acoustic-Emission Quality Control of Plastically Deformed Blanks// Russian Journal of Nondestructive Testing, 2017, Vol. 53, No. 5, pp. 368–377.

[8] Nosov V. V., Matviian I.V., Yamilova A. R. Non-Destructive Evaluation Of Strength Nanofeatures Of Constructional Materials//SMART NANOCOMPOSITE'S letters, Volume 1, Number 1, 2018, pp.53-55.